Response to Reviewer #1:

This paper investigated the relationship between PBLH and surface PM concentrations over China. The interaction between PBLH and surface pollutants under different topographic and meteorological conditions has been carefully considered. However, I have some concerns about the conclusion of the paper. The authors have investigated many parameters that may influence the relationship between PBLH and surface PM concentrations. But all the derived correlations are relatively low. It seems risky to get the strong conclusion based on those correlations.

Response: We are very grateful to the reviewer for his/her valuable comments on our work, which are quite constructive and helpful. We carefully considered all of these comments, and modified some strong conclusion regarding the PBLH-PM relationships, as well as the analysis. Our detailed responses to the reviewer's questions and comments are listed below.

General comments:

1. Page 10. I recommend to put the introduction of MERRA in Section 2, which will make the flow more clear.

Response: Per your kind suggest, we moved the introduction of MERRA data to Section 2 (revised Section 2.2.3).

2. Section 3.1. The authors discussed the differences between CALIPSO and MERRA in detail. Will the differences influence the conclusion about the relationship between PBLH and surface pollutants? If so, how much will it be?

Response: Thanks for this valuable comment. In fact, the reanalysis data take account of large-scale dynamical forcing, and have the ability to produce a general PBLH climatology (Guo et al., 2016) which is used to compare with that derived from CALIPSO in this study. However, the reanalysis data do not consider the impact of aerosols; only limited upper atmospheric measurements are assimilated, and the effects of aerosol-PBL interaction are poorly represented (Ding et al., 2013; Simmons, 2006; Huang et al., 2018). Thus, the reanalysis data offer limited ability to investigate detailed PBLH-PM relationships. Therefore, the observation-based retrievals (CALIPSO PBLH or MPL PBLH) are used to produce the PBLH-PM relationships over China. A detailed discussion has been incorporated into the revised Section 3.1.

3. Section 3.2. The correlation coefficient is very low here (Figure 3). I guess it is too risky to make the statement that PBLH has negative correlation with PM2.5 without conditions, which appeared in both abstract and conclusion.

Response: We greatly appreciate this constructive comment. Indeed, the PBLH is not always negatively correlated with $PM_{2.5}$. The weak correlation coefficients cause some

difficulties in deriving a clear relationship between PBLH and $PM_{2.5}$. In addition to PBLH, $PM_{2.5}$ is also controlled by many other factors (e.g. emissions, wind, synoptic patterns, stability, etc.), and thus, the variation of $PM_{2.5}$ is not necessarily related to PBLH, especially when other factors play dominant roles (e.g. strong wind). In such situations, there are rather weak or uncorrelated relationships between PBLH and $PM_{2.5}$. Strong aerosol-PBL interactions only occur under certain conditions. In our analysis, heavy aerosol loading, plains areas, and weak wind speed would be favorable conditions for relatively strong negative correlations between PBLH and $PM_{2.5}$. This discussion has been incorporated into the revised Section 4.

In addition, we revised the overly strong statements to avoid misleading the reader, and show three examples as follows:

In the abstract, "A generally negative correlation is observed between PM and the PBLH…" has been revised to "Albeit the PBLH-PM correlations are roughly negative for most cases, their magnitude, significance, and even sign vary considerably with location, season, and meteorological conditions."

In conclusion, "We observe widespread negative correlations…" has been revised to "Albeit the PBLH-$PM_{2.5}$ correlations are generally negative for the majority of conditions, their magnitude, significance, and even sign vary greatly by region and timing."

In conclusion, "Strong correlations between PBLHs and aerosols occur in low-altitude regions." has been revised to "The PBLH-$PM_{2.5}$ correlations are found to be more significant in low-altitude regions."

Moreover, we previously used the Pearson correlation coefficient, which is representative in a linear relationship. However, the PBLH-$PM_{2.5}$ relationships are nonlinear under most conditions, and this fact would contribute to the low Pearson correlation coefficients. To partly address this problem, we introduce an inverse function ($f(x) = A/x + B$) to fit the PBLH-$PM_{2.5}$ relationships more closely with set the weighting function as the normalized density. In Figure R1 (the revised Figure 5), we jointly use the regular linear regression and the fitted inverse function to characterize the PBLH-$PM_{2.5}$ relationships. Over North China Plain, the nonlinear inverse function shows high consistency with the average values for each bin, and well represents the behavior of the most dense area in the scatter plot with an improved correlation (correlation coefficient -0.49). Similar improvements in the fitting method are also found in other regions, but are still not significant for Pearl River Delta and Northeast China (relatively clean regions).

The fitting methods are described in the revised Section 2.3. We updated the fitting method description in the revised manuscript, which shows better performance in characterizing the PBLH-$PM_{2.5}$ relationships.

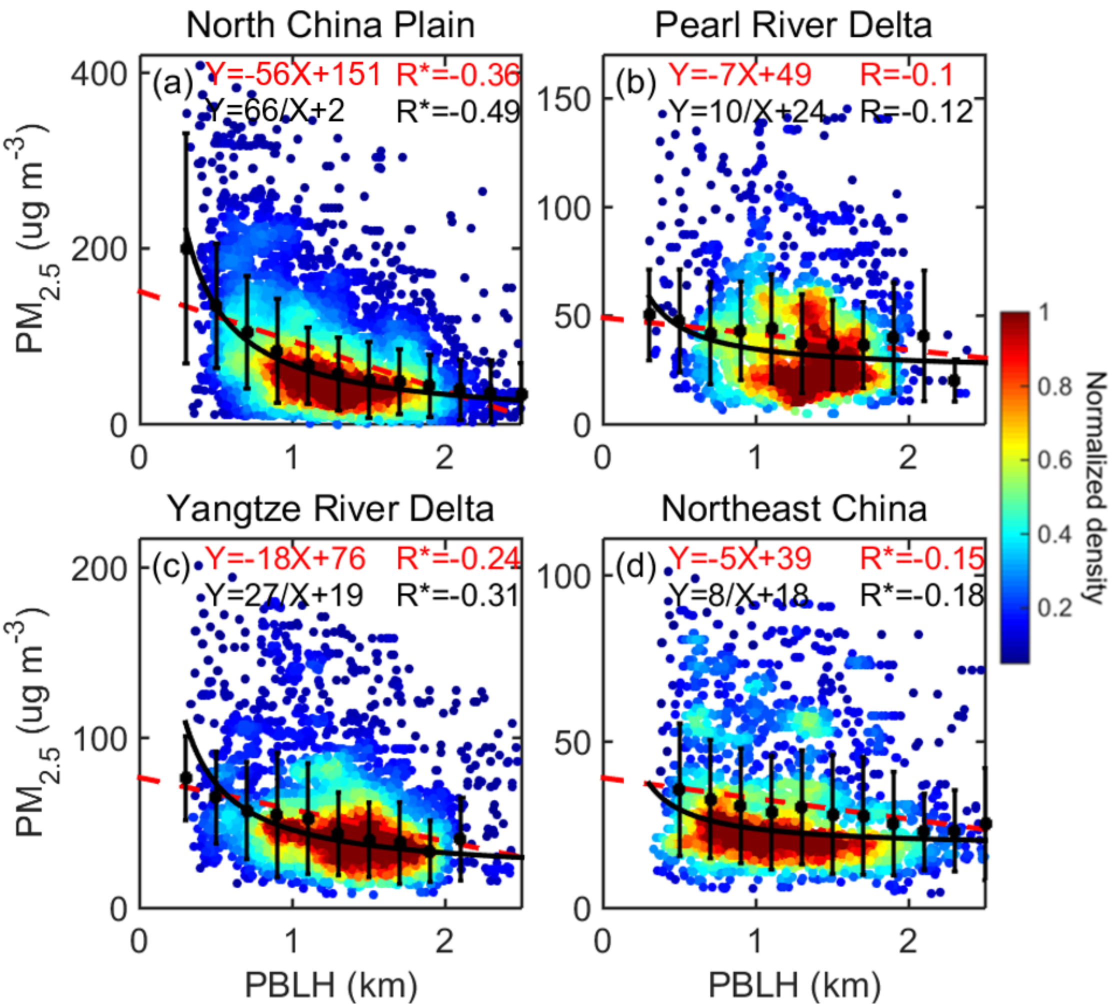

Figure R1. The relationship between CALIPSO-derived PBLH and early-afternoon $PM_{2.5}$ over (a) NCP, (b) PRD, (c) YRD, and (d) NEC. The black dots and whiskers represent the average values and standard deviation for each bin. The red dash lines indicate the regular linear regressions, and the black lines represent the inverse fit ($f(x) = A/_x + B$). The detailed fitting functions are given at the top of each panels, along with the Pearson correlation coefficient (red) and the correlation coefficient for the inverse fit (black). Here and in the following analysis, R with asterisks indicates the correlation is statistically significant at the 99% confidence level. The color-shaded dots indicate the normalized sample density.

4. The authors use many figures in the supplement to support the discussion in the text. Meanwhile, the text is not self-explanatory without the graphs. I suggest the authors to reconsider the arrangement of the whole graphs including what has been included in the manuscript. You may want to delete the description that is not very relative or add some figures that are really necessary.

Response: Thanks for pointing this out. We reorganized the supporting information (SI). Figure S2 was revised to present the $PM_{2.5}$ climatology, and was moved to the main text (the revised Figure 4). Figure S4 was revised to present the relationship between MPL PBLH and $PM_{2.5}$ (or normalized $PM_{2.5}$) at Beijing, and was moved to the main text (the revised Figure 7). Previous Figure S3 and Figure S9 were deleted from the SI. As such, we

believe that our main points are delivered and reflected in the revised main text. The SI presents some additional analyses to complement the points in the main text with more evidences.

5. Section 3.6. I understand the authors would like to perform some preliminary analysis here. But exploring the feedback of absorbing aerosols by only analyzing the correlation between PBLH and PM2.5 looks not convincing for me. You may want to perform some further analysis to make the conclusion more solid or discard this part.

Response: We appreciate your suggestion. Indeed, the analysis in Section 3.6 is insufficient, and we deleted this section as suggested. In the discussion, we mention the feedback of absorbing aerosols would be a potential factor affecting the PBLH-PM relationships, which merits further analysis that will be presented in a future paper, given the long length of the current paper.

6. I suggest the authors to add the applications of the findings in the conclusion. How will the findings influence the model development or policy design in the future?

Response: Per your comment, we added following statement to the Section 4:

"Such information can help improve our understanding of the complex interactions between air pollution, boundary layer, and horizontal transport, and thus, can benefit policy making aimed at mitigating air pollution at both local and regional scales. Our study also contributes to the quantitative understanding of aerosol-PBL interaction and further improvement of surface pollutant monitoring and forecasting capabilities."

Specific comments:

1. *Page 3, line 48, the term of "anthropogenic gases" sounds strange. Anthropogenic emissions?*

Response: We revised the "anthropogenic gases" to "gaseous pollutants".

2. *Page 3, line 49, "they are much more visible". Please clarify what are compared with.*

Response: Per your comment, we revised the statement as "PM pollutants are of greater concern to the public partly because they are much more visible than gaseous pollution…"

3. *Page 6, line 114. The grammar seems not proper.*

Response: Per your kind suggestion, we revised the statement as "These empirical relationships between PBLH and surface pollutants are expected to improve our understanding and forecast capability for air pollution..."

4. *Page 6, line 124. The source of the meteorological data is missing.*

Response: Per your comment, we added the source.

5. *Page 6, line 129. The reason for the usage of "noontime" day is missing.*

Response: Thanks for pointing this out. We changed "noontime" to "early-afternoon" and added some clarifying text:

"To match the CALIPSO retrievals with equator crossings at approximately 1330 local time, we use the surface meteorological and environmental data in early-afternoon, averaged from 1300 to 1500 China standard time (CST). During this period, the PBL is well developed with relatively strong vertical mixing, which is a favorable condition for investigating aerosol-PBL interaction."

6. *Page 11, line 234. The English looks not proper in "The PM2.5 seasonal pattern is generally opposite that of PBLH".*

Response: We revised the statement as "The $PM_{2.5}$ seasonal pattern is generally coupled to that of PBLH…"

7. *Page 11, line 238. The grammar seems not proper.*

Response: We revised the statement as "Both the PBLH and $PM_{2.5}$ also show strong seasonality over NCP. PRD is a relatively clean region, and $PM_{2.5}$ maintains low values (<50 μg m^{-3}) through all seasons"

References:

Guo, J., Miao, Y., Zhang, Y., Liu, H., Li, Z., Zhang, W., He, J., Lou, M., Yan, Y., Bian, L. and Zhai, P.: The climatology of planetary boundary layer height in China derived from radiosonde and reanalysis data. Atmos. Chem. Phys., 16(20), 13,309–13,319. https://doi.org/10.5194/acp-16-13309-2016, 2016.

Huang, X., Wang, Z. and Ding, A.: Impact of Aerosol-PBL Interaction on Haze Pollution: Multi-Year Observational Evidences in North China. Geophysical Research Letters, 2018.

Ding, A. J., et al., Intense atmospheric pollution modifies weather: a case of mixed biomass burning with fossil fuel combustion pollution in eastern China, Atmos. Chem. Phys., 13(20), 10545-10554, 2013.

Simmons, A., ERA-Interim: New ECMWF reanalysis products from 1989 onwards, ECMWF newsletter, 110, 25-36., 2006.

Response to Reviewer #2:

General Comments:

The manuscript studied the relationship between PBLH and PM2.5 concentration over different regions and seasons. Effects of aerosol, winds peed, topography etc. are also included in this study. Many data sources are included, multiple PBLH derived methods are compared, complex statistical relationships are revealed. Thus this study is comprehensive and valuable. While I do have some major revision suggestions since some part of the paper are confusing.

Response: We are very grateful to the reviewer for his/her helpful and constructive comments on our work. All of the comments and concerns raised by the referee have been carefully considered and incorporated into this revision. Our detailed responses to the reviewer's questions and comments are listed below.

Specific Comments:

1) Section 2 is very confusing. I understand that this part describes many observation datasets including ground based (routine and campaign) and satellite. Also includes multiple PBLH derivation methods. Please reorganize the section so that readers can have a very clear idea of the data sources and the purpose of the data. Two subsections of 2.1 Data and 2.2 PBLH derive method is good enough. For Data section, use a table to describe all the data used in this study. I included a sample table here. Current section 2.1 is a description of ground based observations, so CALIPSO related statements (line 126-130) are not fit in here. Please move the sentences to section 2.3 PBLH derived from CALIPSO.

Response: Thanks a lot for the guidance. Following your instruction, we added Table R1 to section 2 to describe the observations from multiple sources and platforms.

Table R1. Description of data.

Observations	Variables	Location	Temporal resolution	Time period
Environmental Stations	$PM_{2.5}$	~1600 sites*	Hourly	01/2012-06/2017
Meteorological Stations	WS/WD	~900 sites**	Hourly	01/2012-06/2017
MPL	PBLH, extinction	Beijing	15seconds	03/2016-12/2017
AERONET	AOD (550nm),	Beijing	~Hourly	01/2016-12/2017
MODIS	AOD	Whole China	Daily	01/2006-12/2017
CALIPSO	PBLH	Orbits in Figure 1d	Daily	06/2006-12/2017
MERRA	PBLH	Whole China	Hourly	01/2006-12/2017

* 224 sites over NCP; 105 sites over PRD; 215 sites over YRD; 159 sites over NEC

** 37 sites over NCP; 92 sites over PRD; 34 sites over YRD; 76 sites over NEC

In addition, we reorganized section 2, and kept two subsections describing the data

and PBLH methodology, respectively. We also added a subsection to illustrate the statistical analysis methods. The CALIPSO-related statements in section 2.1 have been moved to the revised section 2.1.2.

2) PBLH is a fundamental variable in this study. Three observational dataset were used to derive PBL: ground MPL, space borne (CALIPSO), and radiosonde. CALIPSO-PBLH is verified by MPL-PBLH, MPL-PLBH is verified by radiosonde-PBLH. These three PBLH derivation methods have different theory bases which contributes discrepancies among them. Statistics as showed in Figure S1 are important, while please give examples of individual comparisons, e.g. one case of PBLH derivations from all the three observations/methods. Another suggestion is to include illustration figures for PBLH determination processes for both MPL and CALIPSO.

Response: Per your sound suggestion, we updated the statistical analysis for the PBLH comparisons. The RMSE and sample numbers (N) are given in each panel, the correlation coefficients (R) are already given in each panel, and R with asterisks indicates those correlations that are statistically significant above the 99% confidence level. As an example. Figure R1 (the revised Figure S1) show the PBLH retrievals derived from CALIPSO, MPL, and RS on 7 June 2016 over Beijing. Based on aerosol backscatter, CALIPSO and MPL derive consistent PBLH retrievals in this case. Radiosonde also show reasonably good agreement with CALIPSO and MPL retrievals with a difference of ~0.1km.

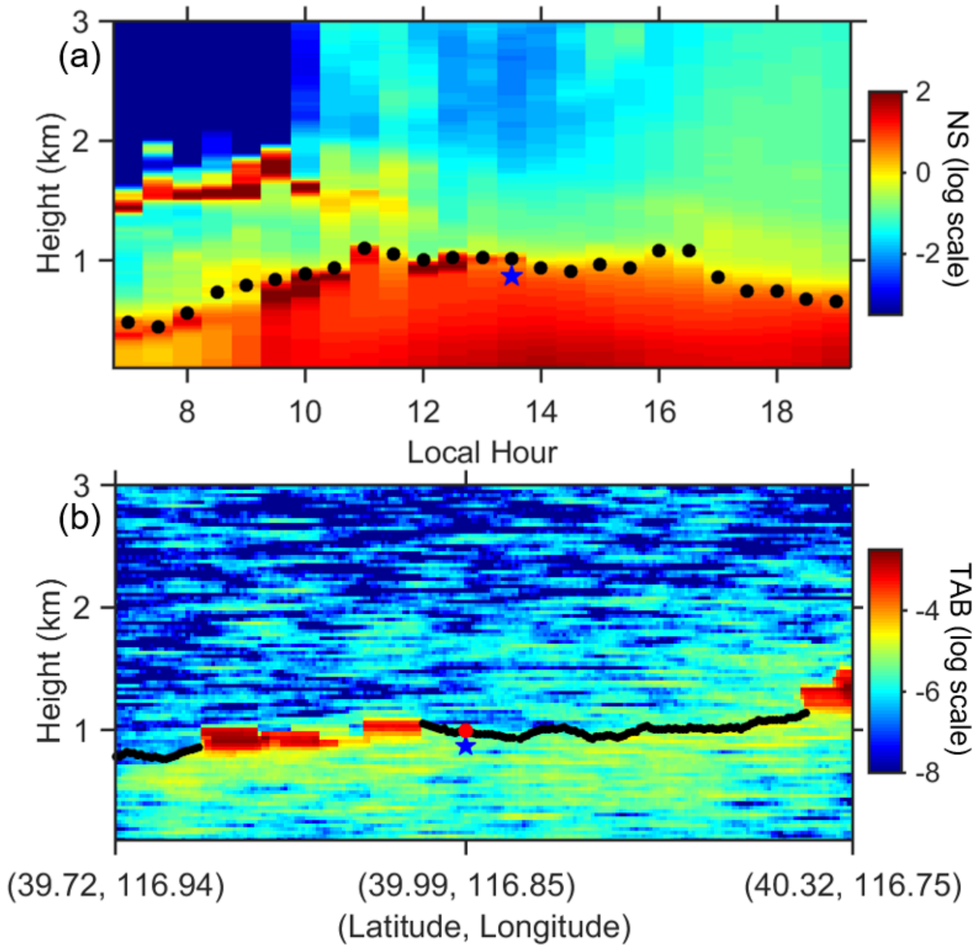

Figure R1. (a) Time evolution of the normalized signal (NS) plot from MPL on 7 June 2016 over Beijing. The black dots identify the PBLH derived from MPL, and the blue star indicates the PBLH derived from radiosonde. (b) Total attenuated backscatter (TAB) plot (log scale) from CALIPSO on 7 June 2016 over Beijing. The black line indicate the PBLH derived from CALIPSO. The red dot represents the corresponding PBLH derived from MPL, and the blue star indicates the PBLH derived from radiosonde.

As CALIPSO provides the primary measurements used in this study, we added a figure illustrating the CALIPSO PBLH determination processes (the revised Figure 2). For retrieving PBLH from MPL, we implement a well-established method, which was developed by Yang et al. (2013) and was adopted in multiple studies (e.g. Lin et al., 2016; Su et al., 2017). The principle is based on the traditional gradient method, and people can access the published paper (Yang et al., 2013) if they seek more details. We might save some space if we do not add the illustration figure for MPL.

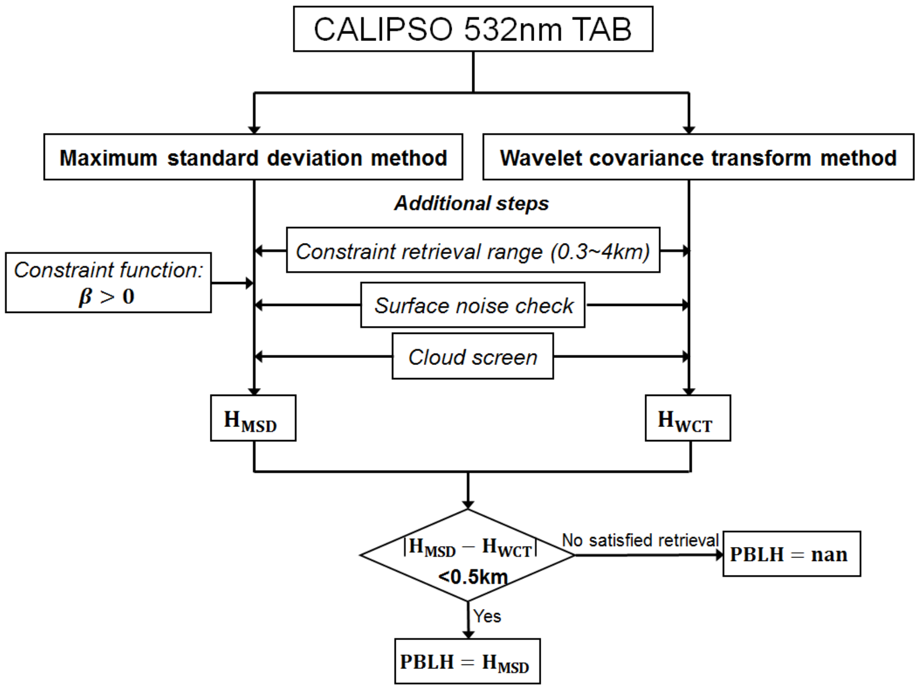

Figure R2. The schematic diagram of retrieving the PBLH from CALIPSO.

3) Section 2.4 MODIS AOD data is suddenly appeared and no explanation of how the data are going to be used and readers have to figure out after read the whole paper. Please add one or two sentences at the beginning to explain the usage.

Response: Thanks for pointing this out; we added the following statements to Section 2 to explain the use of MODIS AOD data:

"Note that aerosol loading is significantly different in different regions. To account for the background pollution level, we normalize the $PM_{2.5}$ with the MODIS AOD to qualitatively account for background or transported aerosol that is not concentrated in the PBL."

4) Line 206-210: please move the brief description of MERRA data to Section 2.

Response: According to your comment, we moved the description of the MERRA data to Section 2 as a new subsection (revised section 2.2.3).

5) Reorganize Figure 2 for easy comparison, suggestion: CALISPO at the left column, corresponding MERRA at the second column.

Response: Per your suggestion, we have revised this figure.

6) Table 1 is very hard to interpret. I suggest to put it in a figure with two y axes, left axis is for PBLH mean and std, right axis for PM2.5. x axis for four regions.

Response: Thanks for this valuable comment. The table is indeed very hard to interpret and conveys little scientific value, and is thus, deleted from the main text but keep as supporting information in case of anyone interested knowing the values of PBLH and $PM_{2.5}$ over different ROIs. We revised Figure 3 and Figure 4 showing the climatological patterns of PBLH and $PM_{2.5}$ that are visually revealing. `

References:

Su, T., Li, J., Li, C., Xiang, P., Lau, A.K.H., Guo, J., Yang, D., and Miao, Y.: An inter-comparison of long-term planetary boundary layer heights retrieved from CALIPSO, ground-based lidar, and radiosonde measurements over Hong Kong. J. Geophys. Res., 122(7), pp.3929-3943, 2017.

Lin, C.Q., Li, C.C., Lau, A.K., Yuan, Z.B., Lu, X.C., Tse, K.T., Fung, J.C., Li, Y., Yao, T., Su, L. and Li, Z.Y.: Assessment of satellite-based aerosol optical depth using continuous lidar observation. Atmospheric environment, 140, pp.273-282, 2016.

Yang, D., Li, C., Lau, A. K. H., and Li, Y.: Long-term measurement of daytime atmospheric mixing layer height over Hong Kong. J. Geophys. Res., 118, 2,422–2,433. https://doi.org/10.1002/jgrd.50251, 2013.

Response to Reviewer #3:

The manuscript investigates relationship between the PBLH and surface PM based on ground-based and onboard lidar, ground environmental and meteorological observations, reanalysis data, and so on. The relationships at different topographic and meteorological conditions over China are specially considered. Although most, if not all, variables show a relatively low correlation with the PBLH, the comprehensive and systematic study reveal the difficulties to drew the relationship between PBLH and surface PM. Generally, the manuscript discusses an important topic, and the methods and discussions are solid and meaningful.

Response: We are very grateful to the reviewer for his/her valuable and constructive comments on our work. All of these comments and concerns raised by the referee have been carefully considered and incorporated into this revision. Our detailed responses to the reviewer's questions and comments are listed below.

General Comments:

1. Some general information about the environmental and meteorological stations used for the four regions should be presented, such as number of stations used in each region, the basic types of them (are them all in the city?). Is there any quality control carried out for the results?

Response: Thanks for the valuable suggestion. We added Table R1 to section 2 to summarize the data. Table R1 not only reports the number of meteorological and environmental stations in each region, but also gives general information about the data used from other sources. The station locations are not all in the cities, but are widely distributed in both urban and rural areas. However, in this large-scale study, we stratify by geographic region, and do not consider the differences between the rural and urban areas specifically.

Table R1. Description of data.

Observations	Variables	Location	Temporal resolution	Time period
Environmental Stations	$PM_{2.5}$	~1600 sites*	Hourly	01/2012-06/2017
Meteorological Stations	WS/WD	~900 sites**	Hourly	01/2012-06/2017
MPL	PBLH, extinction	Beijing	15seconds	03/2016-12/2017
AERONET	AOD (550nm),	Beijing	~Hourly	01/2016-12/2017
MODIS	AOD	Whole China	Daily	01/2006-12/2017
CALIPSO	PBLH	Orbits in Figure 1d	Daily	06/2006-12/2017
MERRA	PBLH	Whole China	Hourly	01/2006-12/2017

* 224 sites over NCP; 105 sites over PRD; 215 sites over YRD; 159 sites over NEC

** 37 sites over NCP; 92 sites over PRD; 34 sites over YRD; 76 sites over NEC

These meteorological and environmental data are routinely measured and quality controlled by government agencies. The $PM_{2.5}$ dataset has been evaluate by other study, and shows relatively high reliability (Liang et al., 2016). There are quality flags along with the meteorological measurements, so error data can be eliminated. These points have been incorporated into the revised Section 3.1.

2. Figure 2 can be reorganized for better comparison. The CALIPSO and MERRA results can be shown in the left and right panel, respectively, and, then, results from the same season can be directly compared.

Response: Per your kind comment, we revised this figure.

3. The MERRA PBLH is not well introduced in the text. Meanwhile, after Figure 2, most results are compared with the CALIPSO results. The MERRA data can be used to evaluate the CALIPSO data, and if they are not used in the discussion for relationship with the PM, why the authors still discuss it in the manuscript.

Response: Thanks for pointing this out. We have added a brief introduction to the MERRA data in Section 2.2.3. As the reanalysis data take account of large-scale dynamic forcing, they are used to produce the climatology pattern of PBLH, and compared with those derived from CALIPSO. We found that the CALIPSO and MERRA retrievals exhibit some mutual features in the seasonality, which is roughly coupled with the seasonal climatology of $PM_{2.5}$. However, we do not focus on the detailed MERRA PBLH values, so we removed the original Table 1 in the main text.

In fact, the reanalysis data bear the model uncertainties, and do not include the impact of aerosols except based on the limited upper atmospheric measurements assimilated (Simmons, 2006). As results, these data poorly represent the effects of aerosol-PBL interactions (Ding et al., 2013; Huang et al., 2018), and offer limited ability to investigate detailed PBLH-PM relationships. As a result, we use only the observation-based retrievals (CALIPSO PBLH or MPL PBLH) to produce the PBLH-PM relationships over China. This discussion has been incorporated into the revised Section 3.1.

4. Section 3.5 and Figure 10 that show the relationship between multiple gases and PBHL are the only part discussing about the gases. Again, relatively poor corrections are obtained, and also considering that this study focuses on the relationship of PBHL and PM, it is not necessary to present those results. This will keep the manuscript more focused.

Response: Per your kind guidance, we deleted this section and Figure 10.

5. Even the relationship between PM and PBLH is relatively weak, how would it possible to further discuss the aerosol absorption feedback in section 3.6.

Response: We deleted this section as suggested, and only mention that the feedback of absorbing aerosols could be a potential influencing factor that merits further analysis.

6. Considering the relatively low correlations shown in the paper, the conclusions are too strong. For example, in the abstract, the authors mentioned that "(line 31) A generally negative correlation is obtained between PM and the PBLH", while the largest correction obtained is only 0.36 from Figure 3. Multiple 'strong correlations' are mentioned in conclusion section.

Response: We appreciate your kind suggestion. Indeed, since $PM_{2.5}$ is controlled by many other factors (e.g. emission, wind, synoptic pattern, stability, etc.), the correlations between PBLH and $PM_{2.5}$ are not very strong under most conditions. We revised the statements in conclusions section to avoid overly strong statements, and state that "Albeit the PBLH-$PM_{2.5}$ correlations are generally negative for the majority conditions, their magnitude, significance, and even sign vary greatly with location, season, and meteorological conditions". We also emphasize that relatively strong PBLH-$PM_{2.5}$ correlations only occurred under certain conditions. According to our analysis, heavy aerosol loading, the plains area, and weak wind speed would be favorable conditions for relatively strong negative correlations between PBLH and $PM_{2.5}$. These points have been incorporated into the revised Section 4.

Moreover, we previously used the Pearson correlation coefficient derived from the linear relationship. However, the PBLH-$PM_{2.5}$ relationships are nonlinear under most conditions, and thus, the nonlinear relationships would contribute to the low Pearson correlation coefficients. To partly address this problem, we included a new fitting method based on an inverse function ($f(x) = A/x + B$) to characterize the PBLH-$PM_{2.5}$ relationships, and set the weighting function as the normalized density. As shown in Figure R1 (the revised Figure 5), the nonlinear inverse function fits show better performance with the data, and characterize the behavior of the most dense area in the scatter plot with improved correlation coefficient (-0.49). Therefore, we include the new fitting method in the revised manuscript, which shows better performance in characterizing the PBLH-$PM_{2.5}$ relationships.

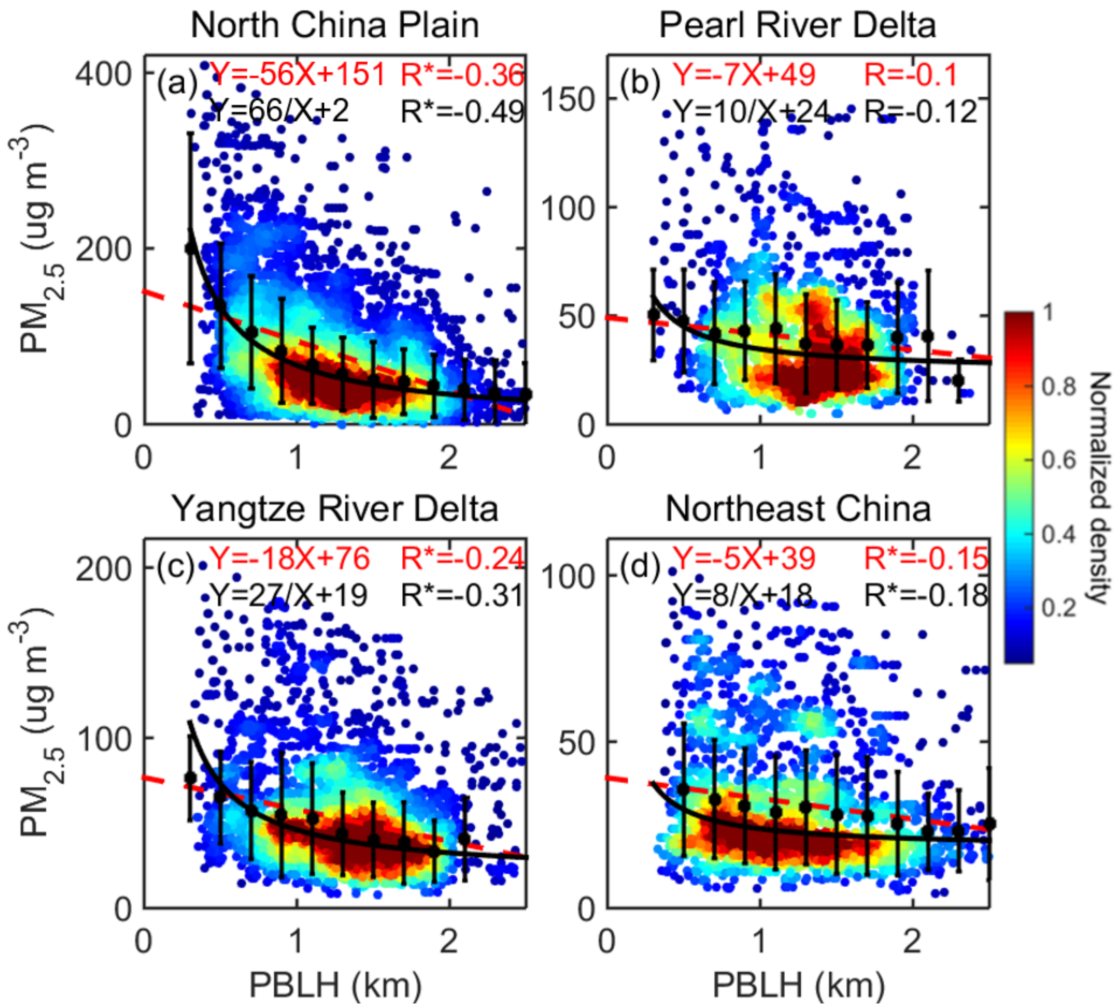

Figure R1. The relationship between CALIPSO-derived PBLH and early-afternoon $PM_{2.5}$ over (a) NCP, (b) PRD, (c) YRD, and (d) NEC. The black dots and whiskers represent the average values and standard deviation for each bin. The red dash lines indicate the regular linear regressions, and the black lines represent the inverse fit ($f(x) = A/x + B$). The detailed fitting functions are given at the top of each panels, along with the Pearson correlation coefficient (red) and the correlation coefficient for the inverse fit (black). Here and in the following analysis, R with asterisks indicates the correlation is statistically significant at the 99% confidence level. The color-shaded dots indicate the normalized sample density.

7. Besides the conclusions, some relatively strong statements in the manuscript should be reconsidered. For example, on line 146, "This method can handle all possible weather conditions and aerosol layers. . .. . .."

Response: Per your kind suggestion, we checked the manuscript and revised or delete these improper statements.

References:

Huang, X., Wang, Z. and Ding, A.: Impact of Aerosol-PBL Interaction on Haze Pollution: Multi-Year Observational Evidences in North China. Geophysical Research Letters, 2018.

Ding, A. J., et al., Intense atmospheric pollution modifies weather: a case of mixed biomass burning with fossil fuel combustion pollution in eastern China, Atmos. Chem. Phys., 13(20), 10545-10554, 2013.

Simmons, A., ERA-Interim: New ECMWF reanalysis products from 1989 onwards, ECMWF newsletter, 110, 25-36., 2006.

Liang, X., S. Li, S. Y. Zhang, H. Huang, and S. X. Chen (2016), PM2.5 data reliability, consistency, and air quality assessment in five Chinese cities, J Geophys Res-Atmos, 121(17), 10220-10236.

Relationships between the planetary boundary layer height and surface pollutants derived from lidar observations over China: R~~r~~egional pattern and influencing~~tial~~ factors

Tianning Su[1], Zhanqing Li[1,2*], Ralph Kahn[3]

[1]Department of Atmospheric and Oceanic Sciences & ESSIC, University of Maryland, College Park, Maryland 20740, USA

[2]State Key Laboratory of Earth Surface Processes and Resource Ecology and College of Global Change and Earth System Science, Beijing Normal University, 100875, Beijing, China

[3]Climate and Radiation Laboratory, Earth Science Division, NASA Goddard Space Flight Center, Greenbelt, MD, USA

∗ *Correspondence to:* Zhanqing Li (zli@atmos.umd.edu)

Abstract. The frequent occurrence of severe air pollution episodes in China has raised great concerns with the public and scientific communitiesbeen a great concern and thus the focus of intensive studies. Planetary boundary layer height (PBLH) is a key factor in the vertical mixing and dilution of near-surface pollutants. However, the relationship between PBLH and surface pollutants, especially particulate matter (PM) concentration, across the whole of China, is not yet well understood. We investigate this issue at ~1600 surface stations using PBLH derived from space-borne and ground-based lidar, and discuss the influence of topography and meteorological variables on the PBLH-PM relationship. Albeit the A generally roughly negative PBLH-PM correlations is observed between PM and the PBLH are roughly negative for most cases,, their magnitudes, significances, and even signs vary considerably with locations, seasons, and meteorological conditionsalbeit varying greatly in magnitude with location and season.. Weak or even uncorrelated PBLH-PM relationships are found over clean regions (e.g. Pearl River Delta), whilewhereas nonlinearly negative responses of PM to PBLH evolution are found over the polluted regions (e.g. North China Plain). Relatively strong PBLH-PM interactions isare found when the PBLH is shallow and PM concentration is high, which typically corresponds to wintertime cases. Correlations are much weaker over the highlands than the plains regions, which may be associated with lower lighter pollution levels loading at higher elevations and a contributions from –mountain breezes. The influence of horizontal transport on surface PM is considered as well, manifested as a negative correlation between surface PM and wind speed over the whole nation. Strong wind with clean upwind sources plays a dominant role in removing pollutants, and leads to weak obscure PBLH-PM correlationrelationships. A ventilation rate is introduced used to jointly consider horizontal and vertical dispersion, which has the largest impact on surface pollutant accumulation over the the North China Plain. In generalAs such, this study is expected tocontributes to

Formatted: Font: 10 pt
Formatted: Font: 10 pt
Formatted: Font: 10 pt
Formatted: Font: 10 pt
Formatted: Font: 10 pt
Formatted: Font: 10 pt
Formatted: Font: 10 pt

improved ~~the~~ understanding of aerosol-PBL interactions and thus ~~the~~our ~~forecast~~ capability of forecasting surface air pollutants. ~~Aerosol absorption feedbacks also appear to affect the PBLH-PM relationship, as revealed via comparing air pollution in Beijing and Hong Kong. Absorbing aerosols in high concentrations likely contribute to the significant PBLH-PM correlation over the North China Plain (e.g., during winter). As major precursor emissions for secondary aerosols, sulfur dioxide, nitrogen dioxide, and carbon monoxide have similar negative responses to increased PBLH, whereas ozone is positively correlated with PBLH over most regions, which may be caused by heterogeneous reactions and photolysis rates.~~

Formatted: Font: Not Bold

Formatted: Indent: First line: 0 cm

1. Introduction

In the past few decades, China has been suffering from severe air pollution, caused by both particulate matter (PM) and anthropogenic gasesgaseous pollutantions. PM pollutants are of greaterst concern to the public partly because they are much more visible than gaseous pollution (Chan and Yao, 2008; J. Li et al., 2016; Guo et al., 2009), and because they have discernible adverse effects on human health. Moreover, airborne particles critically impact Earth's climate through aerosol direct and indirect effects (Ackerman et al., 2004; Boucher et al., 2013; Guo et al., 2017; Kiehl et al., 1993; Li et al., 2016; 2017a).

Multiple factors contribute to the severe air pollution over China. Strong emission due to rapid urbanization and industrialization is a primary cause. MeanwhileIn addition, meteorological conditions and diffusion within the planetary boundary layer (PBL) also play important roles in the exchange between polluted and clean air. Among the meteorological parameters of importance, the PBL height (PBLH) can be related to the vertical mixing, affecting the dilution of pollutants emitted near the ground through various interactions and feedback mechanisms (Emeis and Schäfer. 2006; Seibert et al., 2010; Su et al., 2017a). Therefore, PBLH is a critical parameter affecting near-surface air quality, and it serves as a key input for chemistry transport models (Knote et al., 2015; LeMone et al., 2013). The PBLH can significantly impact aerosol vertical structure, as the bulk of locally generated pollutants tends to be concentrated within this layer. Turbulent mixing within the PBL can account for much of the variability in near-surface air quality. On the other hand, aerosols can have important feedbacks on PBLH, depending on the aerosol properties, especially their light absorption (e.g., black, organic, and brown carbon; Wang et al., 2013). Multiple studies demonstrate that absorbing aerosols tend to affect surface pollution in China through their interactions with PBL meteorology (Ding et al., 2016; Miao et al., 2016; Dong et al., 2017; Petäjä et al., 2016). In a recent comprehensive review, ~~However, the importance and magnitude of aerosol feedback to PBLH are still uncertain, as the feedback is closely related to aerosol structure, and may be weakened by strong turbulence in PBL.~~ Li et al. (2017b) ~~give~~ present~~ed~~ ample evidence~~s~~ of ~~this in a review of the~~such interactions and characterize ~~its~~their determinant factors ~~between the PBL and air pollution~~~~in a recent comprehensive review~~.

There are various methods for identifying the PBLH. ~~The traditional and most common ones are~~ The gradient (e.g., Johnson et al., 2001; Liu and Liang, 2010) and Richardson-~~-~~number methods (e.g., Vogelezang and Holtslag, 1996) are the traditional and most common ones, both of which are typically based on temperature, pressure, humidity, and wind speed profiles obtained by radiosondes. ~~By~~ U~~u~~sing fine-resolution radiosonde observations, Guo et al. (2016) obtained the first comprehensive PBLH climatology over China. Ground-based lidars, such as the micropulse lidar (MPL), are also widely used to derive the PBLH (e.g., Hägeli et al., 2000; He et al., 2008; Sawyer and Li, 2013; Tucker et al., 2009; Yang et al., 2013). The lidar-based PBLH identification relies on the principle that a temperature inversion often exists at the top of the PBL, trapping moisture and aerosols (Seibert et al., 2000), which causes a sharp decrease in the aerosol backscatter signal at the PBL upper boundary. However, using ground-based observations to retrieve the PBLH suffers from poor spatial coverage and very limited sampling. The Cloud-Aerosol Lidar with Orthogonal Polarization (CALIOP) on board the Cloud-Aerosol Lidar and Infrared Pathfinder Satellite Observations (CALIPSO) satellite (Winker et al., 2007), an operational spaceborne lidar, can retrieve cloud and aerosol vertical distributions at a moderate vertical resolution, complementing ground-based PBLH measurements. Several studies already demonstrate both the effectiveness and the limitations of using CALIPSO data for PBLH detection, showing sound but highly variable agreement with those from radiosonde- and MPL-based

PBLH results (Su et al., 2017b; Leventidou et al., 2013; Liu et al., 2015; Zhang et al., 2016).

Several studies have explored the relationship between PBLH and surface pollutants in China. Tang et al. (2016) used ceilometer measurements to derive long-term PBLH behavior in Beijing, further demonstrating the strong correlation between the PBLH and surface visibility under high humidity conditions. Wang et al. (2017) classified atmospheric dispersion conditions~~diffusion conditions~~ based on PBLH and wind speed, and identified significant surface PM changes that ~~also~~ varied with dispersion conditions. ~~{Could be atmospheric stability.}~~ Miao et al. (2017) investigated the relationship between summertime PBLH and surface PM, and discussed the impact of synoptic patterns on the development and structure of the PBL. Qu et al. (2017) derived one-year PBLH variations from lidar in Nanjing, and ~~presented the~~identified a strong correlation between PBLH and PM~~$_{2.5}$~~, especially ~~for~~ on hazy and foggy days.

However, the majority of ~~the~~ studies ~~mostly employ~~considered data from only ~~at~~ a few stations, and as ys~~. Y~~et, the interaction between PBLH and surface pollutants under different topographic and meteorological conditions is not well understood. Assessing the relationship between PM and the PBLH quantitatively over the entire country~~,~~ is of particular ~~significance~~interest. PBL turbulence is not the only factor affecting air quality, so there can be large regional differences in the interaction between the PBLH and PM. As such, the contributions of various factors to the PBLH-PM relationship ~~may be disclosed~~remain uncertain, that thus warrant a further investigation.

Given the above-mentioned limitations, the current~~is~~ study presents a comprehensive exploration of the relationship between the PBLH and surface pollutants over China, for a wide range of atmospheric, aerosol and topographic conditions. Since 2012, China has ~~drastically~~ dramatically increased the number of instruments and implemented rigorous quality control ~~measures~~ procedures ~~to~~

Comment [ZL1]: Needs to define and clarify, because wind is clearly a key factor of dispersion. If so, what do you mean by "also"?

Comment [ST2]: Sorry, there is a misuse of also.

Formatted: Highlight

~~measure~~for hourly pollutant concentration measurements nationally, ~~of~~ providing much better quality data than was previously available. The pollutant data derived from surface observations, along with CALIPSO measurements, offer us an opportunity to investigate the impact of PBLH on air quality on a nationwide basis. Regional characteristics and seasonal variations are considered. Moreover, multiple factors related to the interaction between the PBLH and PM are investigated, including surface topography, horizontal transport, and ~~aerosol type~~pollution level. ~~The relationships between the PBLH and several gas pollutants are also presented. These empirical~~Accounting for the influences ~~of~~ these factors have on the relationships between PBLH and surface pollutants ~~are aimed expected at to improving improve~~will help improve our understanding and ~~forecasting~~ forecast ~~ability~~ capability for air pollution, as well as helping refine meteorological and atmospheric chemistry models.

2. Data and Method

2.1. ~~Data~~ Descriptions of observations

2.1.1. Surface ~~observation sites~~data

The topography of China is presented in Figure 1a, and ~~the~~ pink rectangles outline the four regions of interest (ROI) for the current study: northeast China (NEC), the Yangtze River Delta (YRD), Pearl River Delta (PRD), and North China Plain (NCP). The environmental monitoring station locations are indicated with red dots in Figure 1b. They routinely measure ~~hourly pollutant data, including~~ PM with diameters ≤ 2.5 ~~and 10~~ μm ($PM_{2.5}$ ~~and PM_{10}, respectively~~), which are released to the public in real-time with relatively high credibility (Liang et al., 2016). ~~, sulfur dioxide (SO_2), nitrogen dioxide (NO_2), carbon monoxide (CO), and ozone (O_3).~~ The locations of meteorological stations ~~operated by the China Meteorological Administration~~ are indicated in Figure 1c (data source:

http://data.cma.cn/en). ~~We use~~The wind speed and wind direction at these stations~~data obtained at these stations~~ are quality-controlled and archived by the China Meteorological Administration~~ with the elimination of error and missing data~~. ~~As shown in Figure 1d, blue lines represent the ground tracks over China for the daytime overpasses of CALIPSO. To match the CALIPSO retrievals with surface pollutant and meteorological data, we use the noontime surface data, where "noontime" refers to results averaged from 1300 to 1500 China standard time (CST).~~ We also utilized the MPL data~~ at Beijing~~ and sun-photometer data at Beijing~~ and Hong Kong~~, ~~two~~ a ~~megacities~~ megacity located ~~over~~ within the NCP~~ and PRD respectively~~. The MPL located at Beijing was operated continuously by Peking University (39.99°N, 116.31°E) from Mar 2016 to Dec 2017, with a temporal resolution of 15s and a vertical resolution of 15m. The near-surface blind zones for both lidars are around 150 meters. Background subtraction, saturation, after-pulse, overlap, and range corrections are applied to raw MPL data (He et al., 2008, Yang et al., 2013). In this study, we use Level 1.5 AOD at 550~~/440~~ nm ~~and single scattering albedo (SSA) at 675 nm at~~from the Beijing RADI (40°N, 116.38°E) ~~and Hong Kong PolyU (22.3°N, 114.18°E)~~ Aerosol Robotic Network (AERONET) site,~~s~~ with hourly time resolution ~~are used~~. ~~Since the~~As observations ~~data~~ from multiple sources and platforms are used, we present ~~the~~ descriptions of these observations in Table 1.

2.1.2. CALIPSO data

CALIOP aboard the CALIPSO platform is the first space-borne lidar optimized for aerosol and cloud profiling. As part of the Afternoon satellite constellation, or A-Train (L'Ecuyer and Jiang, 2010), CALIPSO is in a 705-km Sun-synchronous polar orbit between 82°N and 82°S, with a 16-day repeat cycle (Winker et al., 2007, 2009). In this study, we used the CALIPSO data to retrieve the daytime PBLH ~~at~~along its orbit~~s~~. As shown in Figure 1d, blue lines represent the ground tracks over China for

Formatted: Font: Times New Roman, 10 pt

Formatted: Font: Times New Roman, 10 pt

Formatted: Font: Times New Roman, 10 pt

Formatted: Font: Times New Roman, 10 pt

Formatted: Normal, Indent: First line: 0.74 cm the daytime overpasses of CALIPSO. To match the CALIPSO retrievals with equator crossings at approximately 1330 local time, we use the ~~noontime~~ surface meteorological and environmental data in early afternoon~~, where "noontime" refers to results~~ averaged from 1300 to 1500 China standard time (CST). During this ~~noontime~~period, the PBL ~~also~~ is well developed with relatively strong vertical mixing, which is a favorable condition for investigating aerosol-PBL interactions.

2.1.3. MODIS data

The MODIS instruments on board the NASA Terra and Aqua satellites have 2330-km swath widths, and provide daily AOD data with near-global coverage. In this study, we use the Collection 6 MODIS-Aqua level-2 AOD products ~~from the Aqua satellite~~ at 550 nm (available at: https://www.nasa.gov/langley), which is a widely used parameter to represent the columnar aerosol amount. AOD data are archived with a nominal spatial resolution of 10 km × 10 km, and the data are averaged within a 30 km radius around the environmental stations to match with surface PM data. The MODIS land AOD accuracy is reported to be within ±(0.05+15% AERONET AOD) (Levy et al., 2010). Note that~~d~~ ~~the~~ aerosol loading~~s~~ ~~are~~is significantly different ~~for~~in different regions. To ~~take~~ account ~~of~~for the background pollution level, we ~~will utilize the MODIS AOD to~~ normalize the $PM_{2.5}$ with MODIS AOD to qualitatively account for background or transported aerosol that is not concentrated in the PBL.

2.2. ~~PBLH derived from MPL~~Retrieving PBLHs

2.2.1. PBLH derived from MPL

MPL data from Beijing were used to retrieve the PBLH for this study. Multiple methods have been developed for retrieving the PBLH from MPL measurements, such as signal threshold (Melfi et al., 1985), maximum of the signal variance (Hooper and Eloranta, 1986), minimum of the signal profile

Formatted: Font: Times New Roman, 10 pt

Formatted: Font: Times New Roman, 10 pt

Formatted: Font: Times New Roman, 10 pt

Formatted: Font: Times New Roman, 10 pt

Formatted: Normal, Indent: First line: 0.74 cm

Formatted: Font: Times New Roman, 10 pt

Formatted: Font: Times New Roman, 10 pt

Field Code Changed

Formatted: Hyperlink, Font: 10 pt

Formatted: Font: Times New Roman, 10 pt

Formatted: Font: Times New Roman, 10 pt

Formatted: Font: Times New Roman, 10 pt

Formatted: Font: Times New Roman, 10 pt

Formatted: Font: Times New Roman, 10 pt

Formatted: Font: Times New Roman, 10 pt

Formatted: Font: Times New Roman, 10 pt, Subscript

Formatted: Font: Times New Roman, 10 pt

Formatted: Font: Times New Roman, 10 pt derivative (Flamant et al., 1997), and wavelet transform (Cohn and Angevine, 2000; Davis et al., 2000). To derive the PBLH from MPL dataIn this study, we implement a well-established method method, which was developed by Yang et al. (2013), and was adaptedadopted, in multiple studies (Lin et al., 2016; Su et al., 2017a, 2017b).by Yang et al. (2013) to derive the PBLH from MPL data, with a few modificationsadaptations. This method – can handle all possible weather conditions and aerosol layer structures, and is tested to be suitable for processing long-term lidar data. Initially, the first derivative of a Gaussian filter with a wavelet dilation of 60 m is applied to smooth the vertical profile of MPL signals, and to produce the gradient profile. The aerosol stratification structure is indicated by multiple valleys and peaks in the gradient profile. To exclude misidentified elevated aerosol layers above the PBL, the first significant peak in the gradient profile (if one exists) is considered the upper limit in searching for the PBL top. Then, the height of the deepest valley in the gradient profile is attributed to the PBLH; discontinuous or false results caused by clouds are subsequently eliminated manually. In this studyMoreover, we further estimated the shot noise (σ) induced by background light and dark current for each profile, and then added threshold values of $\pm 3\sigma$ to the identified peaks and valleys of this profile to reduce the impact of noise. Figure S1 presents an example of the PBLH retrievals derived from MPL backscatter over Beijing. To validate MPL-derived PBLH, the values are compared with summertime radiosonde PBLH data results at 14:00 CST retrieved by the Richardson number method (e.g., Vogelezang and Holtslag, 1996) at Beijing station (39.80°N, 116.47°E) from potential temperature profiles acquired at Beijing station (39.80°N, 116.47°E) at 14:00 CSTby the Richardson number methods (e.g., Vogelezang and Holtslag, 1996). –Figure S1a S2a shows good agreement (R=~0.7) between MPL- and radiosonde-derived PBLHs over Beijing.

Formatted: Font: Times New Roman, 10 pt, Font color: Black

Formatted: Font: Times New Roman, 10 pt, Font color: Black

Formatted: Font: Times New Roman, 10 pt, Font color: Black

Formatted: Font: Times New Roman, 10 pt, Font color: Black

Formatted: Font: Times New Roman, 10 pt, Font color: Black

Formatted: Indent: First line: 2 ch, Space Before: 10.55 pt, After: 10.55 pt, Don't adjust space between Latin and Asian text, Don't adjust space between Asian text and numbers

2.2.2.2.3. PBLH derived from CALIPSO

CALIOP aboard the CALIPSO platform is the first space-borne lidar optimized for aerosol and cloud profiling. As part of the Afternoon satellite constellation, or A-Train (L'Ecuyer and Jiang, 2010), CALIPSO is in a 705-km Sun-synchronous polar orbit between 82°N and 82°S, with equator crossings at approximately 1330 and 0130 local time and a 16-day repeat cycle (Winker et al., 2007, 2009). CALIOP aboard the CALIPSO platformCALIOP measures the total attenuated backscatter-coefficient (TAB) with a horizontal resolution of 1/3 km and a vertical resolution of 30 m in the low and middle troposphere, and has two channels (532 and 1064 nm). As the nighttime heavy surface inversion and residual layers tend to complicate the identification of the PBLH, we only utilize daytime TAB data (Level 1B) in this study. For retrieving the PBLH from CALIPSO, we typically use the maximum standard deviation (MSD) method, which was first developed by Jordan et al. (2010) and then modified by Su et al. (2017b). In general, it determines the PBLH as the lowest occurrence of a local maximum in the standard deviation of the backscatter profile, collocated with a maximum in the backscatter itself. The PBLH retrieval range (0.3~4km), surface noise check, and removal of attenuating and overlying clouds are subsequently included in this method. In addition, due to the viewing geometry of the instrument, we define a constraint function:

$$\beta(\mathrm{i}) = \max\{f(\mathrm{i}+2), f(\mathrm{i}+1)\} - \min\{f(\mathrm{i}), f(\mathrm{i}-1)\} \ , \qquad (1)$$

where $f(\mathrm{i}+2)$, $f(\mathrm{i}+1)$, $f(\mathrm{i})$, $f(\mathrm{i}-1)$ are four adjacent altitude bins in the 532-nm TAB and where the altitude decreases with increasing bin number i. To eliminate the local standard deviation maximum caused by signal attenuation, we add the constraint $\beta > 0$, and locate the PBLH at the top of the aerosol layer. Moreover, Wwe also use apply the wavelet covariance transform (WCT) method to retrieve the PBLH, and this retrieval serves as a constraint. We eliminate cases when the difference between the MSD and WCT retrievals ~~is above~~exceeds 0.5 km, to increase the reliability of the MSD retrievals. The processes and steps for retrieving PBLH from CALIPSO are summarized in Figure 2. We only analyze ~~the available~~ CALIPSO PBLH retrievals ~~which~~that ~~satisfy~~pass all the indicated tests and constraints. An example of PBLH retrievals derived from CALIPSO is presented in Figure S1.

Due to the high signal-to-noise ratio and reliability of MPL measurements, we use MPL-derived PBLH to test the CALIPSO retrievals. The comparison between CALIPSO- and MPL-derived PBLH at Beijing and Hong Kong (result from Su et al., 2017b) are shown in Figure ~~S1B~~S2b-c. Reasonable agreement between CALIPSO- and MPL-derived PBLHs at these two sites is shown. The correlation coefficients are above 0.6, which is similar to results from previous studies (e.g., Liu et al., 2015; Su et al., 2017b; Zhang et al., 2016). Besides the differences in signal-to-noise ratio, the 10-40 km distance between the MPL station and CALIPSO orbit also contributes to the differences between MPL- and CALIPSO-derived PBLH.

2.2.3. PBLH obtained from MERRA reanalysis data

We ~~will~~ also use the PBLH data obtained from the Modern Era-Retrospective Reanalysis for Research and Applications (MERRA) reanalysis dataset to generate the PBLH climatology with a spatial resolution of 2/3°×1/2° (longitude-latitude). The MERRA reanalysis data uses a new version of the Goddard Earth Observing System Data Assimilation System Version 5 (GEOS-5), which is a state-of-~~-~~the-~~-~~art system coupling a global atmospheric general circulation model (GEOS-5 AGCM) to NCEP's Grid-point Statistical Interpolation (GSI) analysis ~~–~~(Rienecker et al., 2011). Compared~~ing~~ with other reanalysis products (e.g., ECMWF), MERRA PBLHs have relatively high temporal and spatial resolutions~~s~~, and are widely ~~utilized~~used by multiple studies (e.g., Jordan et al., 2010;

Comment [ZL3]: Need to explain what it is used for, and why.

Comment [ST4]: I added related descriptions

Formatted: Indent: First line: 0.63 cm

McGrath-Spangler and Denning., 2012; Kennedy et al., 2011). As the reanalysis data take account of large-scale dynamical forcing, we use MERRA data to generate the PBLH climatology, which further compare with that derived from CALIPSO in this study. The detail discussions can be found in section 3.1.

~~2.,4~~3. ~~MODIS AOD data~~

~~The MODIS instruments on board Terra and Aqua have 2330 km swath widths, and provide daily AOD data with near-global coverage. In this study, we use Collection 6 MODIS level-2 AOD products from the Aqua satellite at 550 nm (available at: https://www.nasa.gov/langley). AOD data are archived with a nominal spatial resolution of 10 km × 10 km, and the data are averaged within 30 km radius around the environmental stations to match with surface PM data. The MODIS land AOD accuracy is reported to be ±(0.05+15% AERONET AOD) (Levy et al., 2010).~~

2.~~4~~3. Statistical Analysis Methods

As a widely used parameter, the Pearson correlation coefficient ~~is~~ derived from ~~the~~a linear ~~fitting~~regression~~,~~ analysis ~~and indicates~~measures ~~how strong is~~the degree to which the data fit~~ness of~~ ~~the~~a linear relationship.~~,s~~ ~~that~~This approach ~~would be~~is ~~invalid.~~less meaningful ~~However, the linear fitting bears limitation forto~~for characteriz~~e~~ing ~~anying the~~ nonlinear relationships. ~~In fact, w~~We find that the PBLH and -PM ~~relationships~~ are correlated but not linearly ~~not ideally linear~~ under most conditions.~~,~~ ~~After trial-and-error analyses, and introduceit is~~We found by trial-and-error that an inverse function ($f(x) = {}^{A}/_{x} + B$) ~~tocan be applied to~~ fits ~~suc~~our data~~h~~ ~~relationships~~ well. Following Winship and Radbill~~.~~ (1994), we ~~can calculate the detail~~derived the fitting~~eding~~ parameters (A and B) and the

Formatted: Font: Font color: Black

Formatted: Indent: First line: 0 cm

Formatted: Indent: First line: 0.63 cm coefficient of determination (R^2) of the PBLH-PM relationship ~~for~~using thise inverse fitting function. Similar to the concept in the linear fitting, we define the slope in the inverse fit~~ting~~ a~~i~~s $-A$. Thus, the slope in linear fit represents the linear slope between PBLH and $PM_{2.5}$, while the slope in inverse fit represents the linear slope between $-\frac{1}{PBLH}$ and $PM_{2.5}$.~~,~~ ~~and the~~The sign of correlation coefficient for the inverse fit~~ting~~ is the same as that of the slope. ~~As a result, we can calculate the correlation coefficient and slope for the inverse fitting.~~ Obviously, ~~for a positive relationship,~~ the correlation coefficient and slope of the inverse fit~~ting~~ for a positive relationship will be positive~~, otherwise, they will be negative~~. Moreover, ~~we can calculate~~ the normalized sample density ~~for~~at each ~~point~~location in a scatter plot ~~to~~ represents the probability distributions in two dimensions (Scott, 2015).~~, and then, set~~Then setting the weighting function in the inverse fit~~ting~~ equal to the normalized density ~~which~~ produces the best-~~-~~fitting results ~~which~~ representing~~s~~ the majority cases. In general, we ~~jointly use~~attempt both ~~the~~ regular linear regression ~~fitting~~ and ~~the~~ inverse fit to characterize the PBLH-PM relationships, and we provide the correlation coefficients and slopes ~~are available~~ for both fitting methods. In each case, t~~T~~he magnitude of correlation coefficient~~s~~ ~~will~~ represents ~~the~~ how well the observationse~~d~~ ~~outcomes~~ are replicated by the fitting model~~s~~, and the magnitude of slope~~s~~ represents the sensitivity of $PM_{2.5}$ to PBLLH changes.

In addition, the statistical significance of the PBLH-PM relationships ~~are~~is tested by two independent statistical methods, namely the least squares regression and the Mann-Kendall (MK) test (Mann, 1945; Kendall, 1975). Least squares regression typically assumes a Gaussian data distribution in the trend analysis, ~~while~~whereas t~~T~~he MK test is a nonparametric test without any assumed functional form,~~ptions~~ and is more suitable for data that do not follow a certain distribution. To improve the robustness of the analysis, a correlation is considered to be significant when the confidence

Formatted: Superscript

Formatted: Subscript

level is above 99% for both least squares regression and the MK test. ~~(~~Hereafter, “significant” indicates the correct ion is statistically significant at the 99% confidence level~~.)~~.

Formatted: Font: Not Bold

3. Results

3.1. Climatological patterns of PBLH and surface pollutants

The climatology of the PBLH, especially its seasonal variability, is very important for air-pollution-related studies. We utilized the CALIPSO measurements ~~during the period~~from 2006 through 2017 to represent the spatial distribution of seasonal mean PBLH with interpolation~~s~~, as shown in Figure ~~2a~~3a-d. A smoothing window of 20 km was applied to the original PBLH data at 1/3 km horizontal resolution~~.~~. ~~For comparison, we also used the PBLH data obtained from the Modern Era-Retrospective Reanalysis for Research and Applications (MERRA) reanalysis dataset with a spatial resolution of 2/3°×1/2° (longitude-latitude). The MERRA reanalysis data uses a new version of the Goddard Earth Observing System Data Assimilation System Version 5 (GEOS-5).~~ The seasonal climatological patterns of MERRA-derived PBLH are presented in Figure ~~2e~~3e-h for the same period. In general, the climatological pattern of MERRA PBLH is similar to that of CALIPSO, though the MERRA values are higher in spring and summer, and the peak values are lower in autumn and winter. Both CALIPSO and MERRA PBLHs are generally shallower in winter, when the development of the PBL is typically suppressed by the weaker solar radiation reaching the surface, and ~~is~~ are generally higher in summer, especially for inland regions.

Note that there are still ~~large~~ considerable differences between the CALIPSO- and MERRA-derived PBLH climatological patterns, which can be attributed to sampling biases, different definitions, and model ~~uncertainty~~uncertainties. First, since the spatial coverage and time resolution are quite different between the CALIPSO and MERRA datasets, the sampling used to calculate the climatologies are quite different. Moreover, MERRA PBLHs are derived from turbulent fluxes computed by the model, whereas CALIPSO usually identifies the top height of an aerosol-rich layer. Although turbulent fluxes would significantly affect aerosol structures, the different definitions still can cause ~~large~~ differences between CALIPSO and MERRA PBLHs. The detailed relationship between of CALIPSO- and MERRA PBLHs is presented in Figure ~~S1D~~S2d. Quantitatively, CALIPSO PBLH values exhibit~~s~~ considerable differences from MERRA results;~~,~~ ~~with a~~the correlation coefficient~~s~~ of ~0.4, indicates~~ing~~ that the observations presented here will likely be useful for future model refinement. ~~In fact, the~~The reanalysis data do take into~~n~~ account ~~of~~ large-scale dynamical forcing, and have the ability ~~of~~ produce~~ing~~ the general PBLH climatology pattern (Guo et al., 2016). However, the reanalysis data do not consider the impact of aerosols ~~but only~~except with limited upper atmospheric measurement data assimilated, ~~and poorly represents~~so the effects of aerosol-PBL interactions are poorly represented (Ding et al., 2013; Simmons, 2006; Huang et al., 2018). Thus, the current reanalysis data have limited ability~~ies~~ ~~for~~to ~~investigating~~support ~~the~~a detailed investigation of PM-PBLH relationships.

Correspondingly, Figure 4 presents the spatial distributions of seasonal mean $PM_{2.5}$ as measured at the surface stations. Both the PBLH and $PM_{2.5}$ over China exhibit large spatial and seasonal variations. The $PM_{2.5}$ ~~shows the opposite~~seasonal pattern is generally coupled~~ing~~ ~~with~~ to that of PBLH;~~,~~ ~~with~~ the lowest values occur in summer and the highest in winter. ~~Since~~ As a high PBLH facilitates the vertical dilution and dissipation of air pollution, the contrasting patterns of PBLH and $PM_{2.5}$ are consistent with expectation. NCP is a major polluted region, with mean $PM_{2.5}$ concentrations overwhelmingly above 100 μg m^{-3} during winter. Both the PBLH and $PM_{2.5}$ also show~~s~~ strong seasonality over NCP. PRD is

Formatted: Font: 10 pt

Formatted: Font: 10 pt

Formatted: Font: 10 pt

Formatted: Font: 10 pt

Formatted: Font: 10 pt

Formatted: Font: 10 pt

Formatted: Font: 10 pt

Formatted: Font: 10 pt

Formatted: Font: 10 pt

Formatted: Font: 10 pt

the a relatively clean region, and $PM_{2.5}$ maintains low values (<50 µg m^{-3}) through all seasons.

As a referenceThe seasonal mean values of CALIPSO and MERRA PBLHs over four ROIs are presented in Table 1. Broadly speaking, the differences between CALIPSO and MERRA PBLHs are much smaller than their standard deviations. PBLH shows strong seasonality over NCP and NEC, ranging from ~0.9 km (winter) to 1.5 km (summer). As the seasonal variation of PBLH is much smaller than the standard deviation over PRD and YRD, the seasonal patterns are not clear for these two regions. MERRA PBLH shows similar seasonal means with CALIPSO over NCP, with differences of ~0.1km, and shows the largest differences (0.5km) with CALIPSO PBLH over NEC during winter.

Correspondingly, the seasonal means and standard deviations of PBLH and $PM_{2.5}$ over four ROIs are listed in Table S1.

Formatted: Subscript

From the seasonal climatologies, we foundfind a coupling pattern between PBLH and The $PM_{2.5}$ seasonal pattern, although one cannot assure theirassume a causal relationship from these plots alone. In subsequent sections, we will utilizeuse the lidar PBLH retrievals from lidars to inverstigateinvestigate the PM-PBLH relationships is generally opposite that of PBLH, with the lowest values in summer and the highest in winter. Since a high PBLH facilitates the vertical dilution and dissipation of air pollution, the contrasting patterns of PBLH and $PM_{2.5}$ are consistent with expectation, although one cannot assure their causal relationship from these plots alone. As this is a major polluted region, both PBLH and $PM_{2.5}$ show particularly strong seasonality over NCP. PRD is a relatively clean region, and $PM_{2.5}$ maintains low values (<50 µg m^{-3}) through all seasons. The spatial distributions of PM_{10}, and multiple gas pollutants (SO_2/NO_2/CO/O_3) climatologies are shown in Figure S2. The seasonal and regional patterns of $PM_{2.5}$, PM_{10}, SO_2, NO_2, and CO all show their highest values in winter and lowest in summer, similar to $PM_{2.5}$. However, unlike the other pollutants, O_3 reaches its

~~highest values during summer. These patterns are discussed~~ in more details ~~in subsequent sections~~.

3.2. Regional relationships between PM and PBLH

If the common factor driving large-scale variations in both PM and PBLH is meteorology, a regional analysis of their relationship could elucidate the meteorological impacts. We investigate the CALIPSO-PBLH and surface $PM_{2.5}$ data case by case. By matching the available CALIPSO retrievals within 35 km of the surface $PM_{2.5}$ observations, we show t~~T~~he scatterplots for ~~annually aggregated~~ PBLH versus surface $PM_{2.5}$ for the four ROIs ~~are shown~~ in Figure ~~3~~5. Despite the overall negative correlations, the correlations between PBLH and $PM_{2.5}$ ~~Although there is~~have ~~a~~ large spreads and ~~regional~~ differences~~, the negative correlations between PBLH and $PM_{2.5}$ are seen in all ROI~~s. Both regular linear regression and inverse fit are applied to characterize the PBLH-PM relationships. ~~As results,~~ ~~S~~significant negative correlations between $PM_{2.5}$ and PBLH are found over NCP with a Pearson ~~PBLH values show the most negative correlation with $PM_{2.5}$ over the NCP, with a~~ correlation coefficient of -0.36~~.~~. In addition, the nonlinear inverse function shows high consistency with the average values for each bin, and ~~well~~ characterizes the PBLH-PM relationship with a somewhat higher correlation coefficient (-0.49). –PBLH also shows significant negative correlation with $PM_{2.5}$ over YRD and NEC, ~~while~~whereas ~~with correlation coefficients of -0.24 and -0.15, respectively. (Hereafter, "significant" indicates the correlation is statistically significant at the 95% confidence level.)~~ t~~T~~he weak PBLH correlation with $PM_{2.5}$ over the PRD is not statistically significant.~~ The relationships between PBLH and PM_{10} are similar to those with $PM_{2.5}$, except with larger spreads, because the magnitudes of PM_{10} are larger than those of $PM_{2.5}$ (Figure S3).~~ The correlation coefficients for the inverse fit are

Formatted: Subscript

Comment [ZL5]: Try to use smaller dots of the data points to see better the distribution pattern by reducing overlapped dots

Comment [ST6]: Changed

generally larger than the Pearson correlation coefficients, ~~and~~ indicating thate the nonlinear fit~~ting~~ may be more suitable for characterizing the PBLH-PM relationships. Such improvements are obvious for NCP and YRD, but are ~~trivial~~not significant over YRD and NEC.~~Compared to CALIPSO data, the MPL has a much higher signal-to-noise ratio and can continuously observe at one location. Therefore, we compare the relationships between MPL-derived PBLH and $PM_{2.5}$ with those from CALIPSO at Beijing (Figure S4). Similar to the relationship derived from CALIPSO, the PBLH shows a significantly nonlinear relationship with $PM_{2.5}$ over Beijing (a major city in the NCP).~~

We not~~ic~~e that the ranges of $PM_{2.5}$ for these ROIs are significantly different; therefore, the background pollution level is likely to be an important factor for the PBLH-PM relationship. We ~~also~~ thus normalize the $PM_{2.5}$ by MODIS AOD, a widely used parameter to represent the total-column~~ar~~ aerosol amount, to qualitatively account for background or transported aerosol that is not concentrated in the PBL. The relationships between PBLH and $PM_{2.5}$/AOD over four ROIs are presented in Figure ~~4~~6. Clearly, after normalizing $PM_{2.5}$ by AOD, the spread of these scatter plots and the regional differences are significantly reduced, and the correlations beco~~a~~me more significant for all ROIs, especially for PRD. This is because transported aerosol aloft can contribute to variability in total column AOD that is unrelated to the PBLH.

Compared to CALIPSO data, the MPL has a much higher signal-to-noise ratio and can continuously observe at one location. Therefore, Figure 7 shows the relationship between MPL-derived PBLH and $PM_{2.5}$ over Beijing (a major city in the NCP), as well as the relationship between PBLH and normalized $PM_{2.5}$. We fi~~ou~~nd the PBLH-PM relationships derived from MPL over Beijing are similar with those derived from CALIPSO over NCP. Probably because of higher data quality, the correlation coefficients for both fitting methods are slightly higher for the relationships derived from surface

Formatted: Subscript

observations than those from CALIPSO. Consistent with the results over NCP, the PBLH shows a significantly nonlinear relationship with $PM_{2.5}$ over Beijing. ~~Since~~As the inverse fitting method better characterizes the PBLH-PM relationships than the regular linear fitting, we only use the inverse fitting method for the PBLH-PM relationships in the main text.

~~Figure S5 provides a closer look at the regional differences among individual sites. As with Figure 3, t~~The most negative correlations between PBLH and $PM_{2.5}$ appear over the NCP, likely a testament to intense PBL-aerosol interactions, which may be caused by concentrated local sources. Comparing with southeast China, absorbing aerosol loading is much ~~higherheavier~~greater over NCP, and may have strong interaction with PBL through the positive feedback (Dong et al., 2017), which may contribute to the significant ~~and~~ nonlinear relationships over NCP. ~~Several scattered sites show positive correlations between PBLH and $PM_{2.5}$, though they are generally not significant.~~ Note that the PBLH-$PM_{2.5}$ correlations are apparently stronger for heavily polluted regions~~,~~ than for clean regions. However, after normalizing $PM_{2.5}$ by AOD, the correlations are improved preferentially for clean regions (where aerosol aloft makes a larger fractional contribution to the total AOD), and thus, the differences between clean and polluted regions are reduced (Figure ~~S6~~S3). It further indicates that the background pollution level plays a critical role in interpreting the PBLH-PM ~~relationship~~observations.

As the NCP experiences the most pronounced seasonality in both PBLH and $PM_{2.5}$, the~~ir~~ relationship over this region also shows the most prominent seasonal differences (Figure S~~5c-f~~4). Figure ~~5~~ 8 focuses on the seasonal dependence of the PBLH and $PM_{2.5}$ relationship over the NCP. The ~~mean~~ magnitude of the slope between $\frac{1}{PBLH}$ and $PM_{2.5}$ for this region is ~90 (unit: km*ug m^{-3}) {Units? Also, the slope changes with PBLH, so is this parameter better described as the curvature?} with a

Comment [ZL7]: Incomplete, than ?

Formatted: Highlight

Comment [ST8]: Directly use the slope between 1/PBLH and PM2.5.

Formatted: Highlight

correlation coefficient of -0.55 ~~μg m^{-3} km^{-1}~~ during winter, and is only ∼~~2~~40 ~~μg m^{-3} km^{-1}~~ in summer. For comparison, the ~~annual~~ seasonally aggregated relationship between PBLH and $PM_{2.5}$ is presented in Figure ~~5e~~8e. $PM_{2.5}$ concentrations do not increase linearly with decreasing PBLH. Specifically, $PM_{2.5}$ increases rapidly with decreasing PBLH when PBLH is lower than 1 km, but changes much more slowly for PBLH > 1.5 km. The seasonal mean values for $PM_{2.5}$ and PBLH are presented as colored dots in Figure ~~5e~~8e, and the whiskers represent the standard deviations. For winter, the PBLH is generally shallow, $PM_{2.5}$ concentrations are high, and thus PBLH shows the most significant negative correlation with $PM_{2.5}$. Conversely, in summer, the PBLH is generally higher, $PM_{2.5}$ concentrations are lower, and the PBLH-$PM_{2.5}$ relationship is virtually flat. Such seasonally distinct PBLH-$PM_{2.5}$ relationships have not previously been studied quantitatively, and ~~can~~ have the potential for ~~contribute to~~ improving $PM_{2.5}$ monitoring and predictions.

3.3. Association with horizontal transport

The PBLH ~~mainly~~ affects mainly the vertical mixing and dispersion of air pollution, but horizontal transport also plays a critical role in surface air quality. Figure ~~6a~~9a-b present the PBLH-$PM_{2.5}$ relationships over China under strong wind (WS>4m s^{-1}) and weak wind (WS<4m s^{-1}) conditions. Under strong wind conditions, $PM_{2.5}$ is found to be much less sensitive to PBLH than for weak wind. In addition, Figure ~~6c~~9c-d show the aerosol extinction profiles as a function of PBLH under strong and weak wind conditions, ~~. The aerosols extinction coefficients are~~as retrieved by the MPLs at Beijing, ~~and~~ with the Klett method ~~is~~ applied (Klett, 1985). ~~Under strong wind conditions, $PM_{2.5}$ is much less sensitive to PBLH than for weak wind.~~ In both strong and weak wind conditions, ~~aerosol structure changes systematically with PBLH, and~~we found ~~sharp~~ clear aerosol extinction

Comment [ZL9]: Isn't "seasonally avaeraged"?

Formatted: Not Superscript/ Subscript

Comment [ZL10]: Aren't contradicting with each other?

gradients appear at the top of the PBL. Nonetheless, under strong wind, the aerosol extinction is typically low in the PBL, and the surface extinction do not change significantly with different PBLH. In this situation, the strong wind likely plays a dominant role in affecting $PM_{2.5}$ concentration by ventilating the PBL. Under weak wind, the response of near-surface pollutants to PBLH is ~~highly~~ more nonlinear, and both aerosol extinction and $PM_{2.5}$ fall rapidly as the PBLH increases from 600m to 1200m.

We further consider the relationship between PBLH-$PM_{2.5}$ under different wind-direction regimes for Beijing. Two different regimes are easy to identify: a northerly wind and a southerly wind; these are divided by the red line in Figure ~~7a~~10a. The northerly air comes from arid and semiarid regions in northwest China and Mongolia, and is usually strong and clean. The southerly wind comes from the southern part of the NCP, with high humidity and aerosol content. To relate the connections between WS, PBLH, and surface air quality, at least qualitatively, ~~we define~~ the ventilation rate (VR) can be represented as VR = WS × PBLH (Tie et al., 2015). Figures ~~7b~~10b-c and d-~~e~~ present the PBLH-$PM_{2.5}$ and VR-$PM_{2.5}$ relationships under southerly wind and northerly wind conditions, respectively. For all wind conditions, VR shows reciprocal relationship with surface $PM_{2.5}$. Under northerly wind conditions, both PBLH-$PM_{2.5}$ and VR-$PM_{2.5}$ relationships are flatter and have lower correlation coefficients. The northerly wind is apparently effective in removing pollutants and may play a dominant role in affecting air quality. For the southerly wind, the $PM_{2.5}$ concentration is highly sensitive to PBLH and VR values.

Comment [ZL11]: If this method was adopted from Tie et al., use of "we define" is misleading.

To further illustrate the coupling effects of PBLH and WS on surface pollutants, Figure ~~8a~~ 11a presents the relationship between ~~noontime~~ early-afternoon WS and $PM_{2.5}$ concentration across China. Overall, WS is negatively correlated with $PM_{2.5}$, although a few stations over southwest China show positive correlations. A negative correlation might be expected in general, as strong winds can be

Comment [ZL12]: May need to change the phrase, c.f. Ralph's comment

Formatted: Font: 10 pt, Not Bold, Font color: Auto effective at removing air pollutants; however, other factors such as wind direction must also be considered, as, for example, upwind sources could increase pollution under higher wind conditions. There are positive correlations between PBLH and near-surface WS in most cases (Figure ~~S7A~~S5a), and thus, low PBLH and weak WS tend to occur together over much of China. These unfavorable meteorological conditions for air quality would exacerbate severe pollution episodes.

To consider horizontal and vertical dispersion jointly, we investigate the nationwide relationships between VR and $PM_{2.5}$. In general, VR is overwhelmingly negative correlated with surface $PM_{2.5}$ (Figure ~~S7b~~S5b). Based on Figure ~~8a~~10, VR is typically reciprocal to $PM_{2.5}$ for ~~all~~ different wind conditions, and thus, we use the function ~~$f(x)$~~$VR = {}^{A}/_{PM_{2.5}}$~~x~~ to characterize the relationship between VR and $PM_{2.5}$, with A as the fitting parameter~~, and x is VR, and $f(x)$ is $PM_{2.5}$~~. The spatial distribution of A, presented in Figure ~~8b~~11b, shows the largest values over the NCP, indicating that the $PM_{2.5}$ concentration is highly sensitive to the VR there. Moreover, VRs are relatively large over the coastal areas, where sea-land breezes could play a role in dispersing air pollution. The detailed relationships and fitting functions for four ROIs are presented in Figure ~~S8~~S6. We note that although there are large regional differences in the PBLH-$PM_{2.5}$ relationship (Figure ~~3~~5), the VR-$PM_{2.5}$ relationships are similar for the different study regions. Therefore, by combining vertical and horizontal dispersion conditions, the overall VR apparently has a similar effect on $PM_{2.5}$ for all four ROI.

Comment [ZL13]: Use the term directly in the equation, e.g. PM2.5=A/VR

Comment [ST14]: Changed

Comment [ZL15]: Figure resolution is too coarse. Use high-r figures to make them look much sharper !

Comment [ST16]: I re-plot this figure.

3.4. Correlations with topography

The PBL structure and $PM_{2.5}$ concentration can both be affected by topography. We ~~also~~ divided ~~all~~ the sites into two categories based on elevation: plains (elevation < 0.5 km) and highland (elevation > 1 km). Figure ~~9a~~12a-d presents the correlation coefficients and slopes in the inverse fit between $PM_{2.5}$

and PBLH for the plains and highland areas. {I keep wondering whether “slope” is really the right word for the fitting parameter in the inverse relationship. I think it might be misleading.} For calculating the correlation coefficient and slope, we require that the matched sampling number of matched CALIPSO PBLH and $PM_{2.5}$ samples is larger than 15 infor each site. Much stronger higher correlation coefficients exist are found in the plains than the highlands., and the slope (i.e. linear slopes between $-\frac{1}{\text{PBLH}}$ and $PM_{2.5}$) in the plains is ~3 times that in highlands. A reciprocal correlation relationship is shown between station elevation and the PBLH-$PM_{2.5}$ slope between $-\frac{1}{\text{PBLH}}$ and $PM_{2.5}$ (Figure 9e12e). The magnitudes of slopes decrease dramatically with elevation increase, for elevations between 0 and 500 m. Local emissions also affect aerosol loading, and differences between plains and highland areas regarding local source activity could be important here as well. Figure 9e 12e shows that the low-elevation regions are typically more polluted than highland areas, and the magnitudes of the PBLH-$PM_{2.5}$ slopes alsoslopes tend to be higher. Here, we utilized the inverse fitting method to reveal the different PBLH-PM relationships betweenfor the plains and highland areas, whileand we can find the similar conclusion by using the linear fitting method (Figure S7).

Returning to Figure S5S3, much stronger correlations for PBLH-$PM_{2.5}$ relationships are found over polluted regions, which also correspond to the plains areas, due to strong local emissions. Therefore, high aerosol loading is likely to be another factor contributing to the strong correlation between PBLH and $PM_{2.5}$ over the plains, whereas the low $PM_{2.5}$ concentration may contribute to the weak PBLH- $PM_{2.5}$ correlation over the highlands.

In addition, horizontal transport is associated with topography. Thus, we illustrate the distribution of WS for plains and highland areas in Figure 9f12f. Clearly, WS is generally larger for highland areas, especially for the strongest wind cases. In fact, the 10% and 25% quantiles of WS are nearly the

Formatted: Highlight

Formatted: Highlight

Comment [ST17]: Yes, it may cause some misunderstanding. We may still use the term of “slope” here, but clarify that the slope represents the linear slope between $-\frac{1}{\text{PBLH}}$ and $PM_{2.5}$, which is a constant (-A in the inverse fit). We point out when we use this term in both text and figure caption, and thus, the readers won’t be misled based on our definition.

Formatted: Highlight

Formatted: Subscript

same between plains and highland areas, whereas there are apparent clear differences in the 75% and 90% quantiles. Strong wind cases account for 37% of the total over highland areas, and but only account for 27% of the total over the plains. As discussed in section 3.3, strong wind can effectively remove surface pollutants, and can play a dominant role in affecting determining local pollution levels. In this situation, PBLH might not play as critical a role in PM concentration. Thus, mountain slope winds, along with less local emission, are likely to be leading factors accounting for the differences in PBLH-$PM_{2.5}$ correlations between plains and highland areas.

3.5. Correlations between gaseous pollutants and PBLH

Secondary aerosol contributes significantly to the surface PM concentration over China (Huang et al., 2014). Multiple gas pollutants, such as SO_2, NO_2, and CO, are major precursor emissions for the formation of secondary aerosols, which are closely related to $PM_{2.5}$ concentration (Guo et al., 2014; Wang et al., 2016). Further, the near surface concentrations of these gaseous pollutants can also have severely negative effects on the environment and human health. We investigate the relationships between gaseous pollutants and the PBLH due to their importance, by matching the CALIPSO PBLH with SO_2/NO_2/CO/O_3 concentrations obtained from surface stations (Figure 10). Again, the relationships between CALIPSO PBLH and SO_2/NO_2/CO/O_3 are similar to those derived from MPLs (Figure S4). For SO_2, NO_2, and CO, the correlations with PBLH are similar to the PBLH-PM correlations over NCP, but slightly weaker.

Similar to PBLH-PM relationships, the correlations between PBLH and SO_2/NO_2/CO are negative for all ROIs. This is understandable, because the PBLH is likely to play a role in the vertical dilution and dissipation of most gaseous pollutants. However, O_3 shows a positive correlation with PBLH for all

ROIs, which might be due to O_3 photochemistry. As radiation reaching the surface increases, convection is enhanced and the PBLH tends to grow higher. At the same time, increased insolation with sufficient precursor emissions (NO_x, CO, and VOCs) can increase the net photochemical production of O_3. Therefore, higher O_3 concentrations and high PBLH could occur together. Moreover, when the PBL is shallow and aerosol concentration is high, heterogeneous reactions on surfaces of multiple aerosols (e.g. sulfate, mineral dust, and organic carbon aerosols) can uptake ozone precursors such as NO_x and N_2O_5, and thus, reduce the ozone production (Ravishankara, 1997; Jacob., 2000). And Liao and Seinfeld (2005) found that the high aerosol loading reduces ozone concentrations by 25-30% through heterogeneous reactions over eastern China. Taken together, decreased PBLH correlates with increased near-surface aerosol concentration, leading to a reduction in precursors required for O_3 production, and an increase in O_3 destruction by heterogeneous reactions. This could explain, at least qualitatively, the positive PBLH-O_3 relationship.

3.6. Potential feedback of absorbing aerosols

Depending on their radiative properties, aerosols can have feedbacks on the PBLH. Multiple studies point out a positive feedback between absorbing aerosols and the PBLH (Ding et al., 2016; Miao et al., 2016; Petäjä et al., 2016). Using lidars and AERONET data, we examine the link between the PBLH-$PM_{2.5}$ relationship and particle optical properties over Beijing and Hong Kong. We utilized AERONET SSA data to classify aerosols as absorbing (SSA ≤ 0.85) or weakly absorbing (SSA > 0.9). The correlation between PBLH and $PM_{2.5}$ is much stronger for absorbing cases over both Beijing and Hong Kong (Figure 11). Noted the PBLHs over Beijing are obtained from MPL. Due to lack of available MPL data, the PBLHs over Hong Kong are calculated by CALIPSO. Since AERONET SSA is more reliable for the cases when AOD at 440nm is above 0.4 (Schafer et al., 2014), Figure S9 shows the PBLH-$PM_{2.5}$ relationship for absorbing and weakly absorbing cases over Beijing with a constraint of AOD_{440}>0.4. The PBLH-$PM_{2.5}$ correlation remains considerably stronger for absorbing than weakly absorbing cases. Under sufficient aerosol loading, we found PBLH-$PM_{2.5}$ correlations become stronger for both absorbing and weakly absorbing cases. In addition, there are many more strongly absorbing cases for Beijing (~35%) than for Hong Kong (~10%), and the total PBLH-$PM_{2.5}$ correlation is much stronger over Beijing.

Moreover, we show how absorbing optical depths over Beijing and Hong Kong correlate with the general PBLH-$PM_{2.5}$ relationship in Figure 11e-f. Under highly absorbing optical depth conditions, $PM_{2.5}$ tends to be higher for a given PBLH. Large absorbing optical depths in Beijing offer great potential for reducing the radiation reaching the surface, likely reducing the PBLH, and at the same time, heating the middle and upper PBL, which would tend to cause a temperature inversion and increase the stability in the PBL. The strongly absorbing aerosols with high loading are likely to give important feedback to PBLH, and may contribute to the strong correlation between the PBLH and PM over Beijing. Other factors could be involved, such as the vertical distribution of aerosol, the insolation, and the actual SSA of the particles; further examination of these phenomena is beyond the scope of the current paper.

Other factors could be come into play as wellbe involved, such as the vertical distribution of aerosol, the insolation, and the actual SSA of the particles; further examination of these phenomena is beyond the scope of the current paper.

4. Discussion and conclusions

Based on ten years of CALIPSO measurements and other environmental data obtained from more than 1500 stations, large-scale relationships between PBLH and $PM_{2.5}$ are assessed over China. AlbeitAlthough the the PBLH-$PM_{2.5}$ correlations are being generally negative for the majority of conditions, PBLH-$PM_{2.5}$ correlations for majority conditions, their magnitudes, significances, and even signs of the PBLH-$PM_{2.5}$ correlations for majority conditions, vary greatly with locations, seasons, and meteorological conditionsWe observe widespread negative correlations, albeit varying greatly in magnitude and seasonal timing by region.. Nonlinear responses of $PM_{2.5}$ to PBLH evolution are found under some conditions, especially for NCP, the most polluted region of China.. We further usedapplied an inverse function ($f(x) = {}^{A}/_{x} + B$) to characterize the PBLH-$PM_{2.5}$ relationships with overall better performance than a linear regression. Partly due to Tthe nonlinear relationship, relatively strongStrongest ofbetween PBLH and -$PM_{2.5}$ shows stronger interaction is found when the PBLH is shallow and $PM_{2.5}$ concentration is high, which typically corresponds to the wintertime cases. Specifically, the negative correlation between PBLH and $PM_{2.5}$ is most significant during winter. Moreover, we find that regional differences in the PBLH-$PM_{2.5}$ relationships are correlated with topography. Strong The PBLH-$PM_{2.5}$ correlations isare found to be more significant between PBLHs and aerosols occur in low-altitude regions. This might be related to the more frequent air stagnation and strong local emission over China's plains, as well as a greater concentration of emission sources. The mountain breezes and a larger fraction of transported aerosol above the PBL help contribute to weakening the PBLH-$PM_{2.5}$ correlation over highland areas.

Note thatd the PBLH-$PM_{2.5}$ relationships are not necessarilyalways be significant nor negative (Geiß et al., 2017). In addition to PBLH, $PM_{2.5}$ is also controlledaffected by many other factors, such as (e.g. emissions, wind, synoptic patterns, atmospheric stability, etc.). In some situations (e.g. strong wind and low aerosol loading), PBLH woulddoes not play a significantdominant role in modulating surface

Formatted: Font: 10 pt, Not Bold, Font color: Auto

Formatted: Font: 10 pt, Not Bold, Font color: Auto

Formatted: Font: 10 pt, Not Bold

Formatted: Font: 10 pt, Not Bold

Formatted: Font: 10 pt, Not Bold

Formatted: Font: 10 pt, Not Bold

Formatted: Font: 10 pt, Not Bold

Formatted: Font: 10 pt, Not Bold

Formatted: Font: 10 pt, Not Bold

pollutants, and result in the weak or uncorrelated relationships between PBLH and $PM_{2.5}$. A common feature is the Wweak PBLH-$PM_{2.5}$ correlations is a common feature over relatively clean regions. Due to the importance of regional pollution levels, we normalized $PM_{2.5}$ by MODIS total-column AOD to account for the background aerosol in different regions. Comparing to PBLH-$PM_{2.5}$ correlations, the correlations between PBLH and normalized $PM_{2.5}$ ($PM_{2.5}$/AOD) increased significantly for clean regions, resulting in smaller regional differences overall. Retrieving surface $PM_{2.5}$ from AOD constraints has been investigated in many studies. The detailed relationships between PBLH and $PM_{2.5}$/AOD over different ROIs are also expected to be significant for relating $PM_{2.5}$ to remotely sensed AOD, due to the way PBLH affects near-surface aerosol concentration.

Horizontal transport also shows significant inverse correlation with $PM_{2.5}$ concentrations. WS and PBLH tend to be positively correlated with each other in the study regions, which means meteorologically favorable horizontal and vertical dispersion conditions are likely to occur together. Wind direction can also significantly affect the PBLH-PM relationship. Strong wind with clean upwind sources plays a dominant role in improving air quality over Beijing, for example, and leads to weak PBLH-PM correlation. The combination of WS and PBLH, representing a “ventilation rate,” shows a reciprocal correlation with surface PM in all the regions studied. VR also is found to have the largest impact on surface pollutant accumulation over the NCP.

As major precursor emissions for secondary aerosols, SO_2, NO_2, and CO show negative correlations with PBLH, similar to the PBLH-PM correlations. However, O_3 is positively correlated with PBLH over most regions, which may be caused by heterogeneous reactions and photolysis rates. This observation merits further investigation using comprehensive measurements of chemical properties together with necessary simulations from atmospheric chemistry model to ascertain the

Formatted: Font: 10 pt, Not Bold

Formatted: Subscript

Formatted: Font: Font color: Black

Formatted: Indent: First line: 0.63 cm, Space Before: 0 pt, After: 0 pt causes of the positive PBLH-O_3 correlations.

The feedback of absorbing aerosol also is a potential factor for affecting the PBLH-$PM_{2.5}$ relationships. Compareding with southeast China (e.g. PRD), the absorbing aerosol loading is much higher over NCP, and is reported to have strong interaction with PBL viae thea positive feedback in this region (Dong et al., 2017; Ding et al., 2016; Huang et al., 2017). Such conclusions are consistentd with our results, that show of the significant PBLH-$PM_{2.5}$ correlations over NCP and weak correlations over PRD. The important feedback of absorbing aerosols may also contribute to the nonlinear relationship between PBLH and $PM_{2.5}$.

Formatted: Subscript

As revealed by observations at Beijing and Hong Kong, absorbing aerosols with sufficient aerosol loading likely contribute the strong PBLH-PM correlation. Large absorbing AOD would reduce the radiation reaching the surface and heat the middle and upper PBL, which could increase the stability in the PBL, representing a direct interaction between PBLH and PM. Much more strongly absorbing cases for NCP than for PRD appear to contribute to the large contrast for PBLH-PM correlations between these two regions. On the other hand, despite the strong correlations for absorbing cases with sufficient aerosol loading, identifying a causal relationship between them is still elusive, as confounding factors, such as aerosol vertical distribution, aerosol microphysical properties, ambient insolation, and meteorological conditions, could all be involved. This issue merits further analysis using more comprehensive measurements from field experiments, from which integrated aerosol conditions and model simulations can account for aerosol radiative forcing while controlling for all the other relevant variables.

Our work comprehensively covers the relationships between PBLH and surface pollutants over large regional~~r~~ spatial scales in China. Multiple factors, such as background pollution level, horizontal transport, and topography~~, and aerosol optical properties~~, are found to be highly correlated with PBLH and near-surface aerosol concentration. Such information can help improve our understanding ~~for~~ of the complex interactions between air ~~pollution~~ pollution, boundary layer depth, and horizontal transport, and thus, can benefit ~~for the~~ policy making ~~of~~aimed at mitigating the air pollution~~s~~ ~~in~~at both local and regional scales. ~~The~~Our findings ~~of oOur study also would be beneficial for~~provide ~~a~~ deeper insight, and ~~help gain more~~contribute to the quantitative~~ly~~ understanding of~~,~~ aerosol-PBL interactions, which could help in refining meteorological and atmospheric chemistry models. ~~and further improving the monitoring and~~ ~~which~~Further, this work may ~~be beneficial to~~ enhance surface pollution monitoring and ~~the~~ forecasting capabilit~~ies~~y~~, of surface pollution~~~~ants~~.

Data availability. The meteorological data are provided by the data center of China Meteorological Administration (data link: http://data.cma.cn/en). The hourly $PM_{2.5}$ data are released by the Ministry of Environmental Protection of the People's Republic of China (data link: http://113.108.142.147:20035/emcpublish) and Taiwan Environmental Protection Administration (data link: http://taqm.epa.gov.tw). The CALIPSO and MODIS data are obtained from the NASA Langley Research Center Atmospheric Science Data Center (data link: https://www.nasa.gov/langley). The MERRA reanalysis data are publicly available at https://disc.sci.gsfc.nasa.gov/datasets?page=1&keywords=merra. The AERONET data are publicly available at https://aeronet.gsfc.nasa.gov.

Competing interests. The authors declare that they have no conflict of interest.

Acknowledgements. This work is supported in part by grants from the National Science Foundation (NSF) (AGS1534670) and NSF of China (91544217). The authors would like to acknowledge the Department of Atmospheric and Oceanic Sciences of Peking University for providing the ground-based lidar data. We thank ~~the~~ Prof. Chengcai Li and Prof. Jing Li for theirs effort in establishing and maintaining the MPL site. We thank Prof. Zhengqiang Li for his effort in establishing and maintaining the Beijing RADI AERONET site. We greatly appreciate the helpful advice from Prof. Jing Li and Prof. Chengcai Li at Peking University. We thank the provision of surface pollutant data by the Ministry of Environmental Protection of the People's Republic of China and Taiwan Environmental Protection Administration, and also thank the provision of meteorological data by China Meteorological Administration. We extend sincerest thanks to the CALIPSO, MODIS~~, AERONET,~~ , and MERRA teams for their datasets. The contributions of R. Kahn are supported in part by NASA's Climate and Radiation Research and Analysis Program under H. Maring, NASA's Atmospheric Composition Modeling and Analysis Program under R. Eckman.

Formatted: Font: Times New Roman, 10 pt

Formatted: Font: Times New Roman, 10 pt

Formatted: Font: Times New Roman, 10 pt

Formatted: Font: Times New Roman, 10 pt

Formatted: Indent: First line: 0.74 cm

Formatted: Font: Not Italic

References

Ackerman, A. S., Kirkpatrick, M. P., Stevens, D. E., and Toon, O. B.: The impact of humidity above stratiform clouds on indirect aerosol climate forcing. Nature, 432, 1,014–1,017. https://doi.org/10.1038/nature03174, 2004

Boucher, O., Randall, D., Artaxo, P., Bretherton, C., Feingold, G., Forster, P., Kerminen, V.M., Kondo, Y., Liao, H., Lohmann, U. and Rasch, P.: Clouds and aerosols. In Climate Change 2013: The Physical Science Basis. Contribution of Working Group I to the Fifth Assessment Report of the Intergovernmental Panel on Climate Change. (pp. 571–657). Cambridge Univ. Press, Cambridge, U. K. and New York, NY, USA, 2013.

Cai, Y. F., Wang, T. J., Xie, M., and Han, Y.: Impacts of atmospheric particles on surface ozone in Nanjing. Climatic and Environmental Research, 18, 251–260, 2013.

Chan, C. K. and Yao, X.: Air pollution in megacities in China. Atmos. Environ., 42, 1–42. https://doi.org/10.1016/j.atmosenv.2007.09.003, 2008.

Cohn, S. A. and Angevine, W. M.: Boundary layer height and entrainment zone thickness measured by lidars and wind-profiling radars. Journal of Applied Meteorology, 39, 1,233–1,247. https://doi.org/10.1175/1520-0450(2000)039<1233:BLHAEZ>2.0.CO;2, 2000.

Davis, K. J., Gamage, N., Hagelberg, C. R., Kiemle, C., Lenschow, D. H., and Sullivan P. P.: An objective method for deriving atmospheric structure from airborne lidar observations. J. Atmos. Oceanic Technol., 17(11), 1,455–1,468. https://doi.org/10.1175/1520-0426(2000)017<1455:AOMFDA>2.0.CO;2, 2000.

Deng, X., Zhou, X., Tie, X., Wu, D., Li, F., Tan, H. and Deng, T.: Attenuation of ultraviolet radiation reaching the surface due to atmospheric aerosols in Guangzhou. Science Bulletin, 57(21), 2,759–2,766. https://doi.org/10.1007/s11434-012-5172-5, 2012.

Ding, A. J., et al., Intense atmospheric pollution modifies weather: a case of mixed biomass burning with fossil fuel combustion pollution in eastern China, Atmos. Chem. Phys., 13(20), 10545-10554, 2013.

Ding, A. J., X. Huang, W. Nie, J. N. Sun, V.-M. Kerminen, T. Petäjä, H. Su, Y. F. Cheng, X.-Q. Yang, M. H. Wang, X. G. Chi, J. P. Wang, A. Virkkula, W. D. Guo, J. Yuan, S. Y. Wang, R. J. Zhang, Y. F. Wu, Y. Song, T. Zhu, S. Zilitinkevich, M. Kulmala, C. B. Fu.: Enhanced haze pollution by black carbon in megacities in China. Geophys. Res. Lett., 43, 2,873–2,879. https://doi.org/10.1002/2016GL067745, 2016.

Dong, Z., Li, Z., Yu, X., Cribb, M., Li, X., and Dai, J.: Opposite long-term trends in aerosols between low and high altitudes: a testimony to the aerosol–PBL feedback. Atmos. Chem. Phys., 17(12), 7,997–8,009. https://doi.org/10.5194/acp-17-7997-2017, 2017.

Emeis, S. and Schäfer, K.: Remote sensing methods to investigate boundary-layer structures relevant to air pollution in cities. Boundary Layer Meteorol., 121(2), 377-385, 2006.

Flamant, C., Pelon, J., Flamant, P. H., and Durand, P.: Lidar determination of the entrainment zone thickness at the top of the unstable marine atmospheric boundary layer, Boundary-Layer Meteorology, 83(2), 247–284. https://doi.org/10.1023/A:1000258318944, 1997.

Guo, J., Miao, Y., Zhang, Y., Liu, H., Li, Z., Zhang, W., He, J., Lou, M., Yan, Y., Bian, L. and Zhai, P.: The climatology of planetary boundary layer height in China derived from radiosonde and

Formatted: Indent: Left: 0 cm, First line: 0 ch

reanalysis data. Atmos. Chem. Phys., 16(20), 13,309–13,319. https://doi.org/10.5194/acp-16-13309-2016, 2016.
Guo, J., Su, T., Li, Z., Miao, Y., Li, J., Liu, H., Xu, H., Cribb, M. and Zhai, P.: Declining frequency of summertime local-scale precipitation over eastern China from 1970 to 2010 and its potential link to aerosols. Geophys. Res. Lett., 44(11), 5,700–5,708. https://doi.org/10.1002/2017GL073533, 2017.
Guo, J.P., Zhang, X.Y., Che, H.Z., Gong, S.L., An, X., Cao, C.X., Guang, J., Zhang, H., Wang, Y.Q., Zhang, X.C. and Xue, M., 2009. Correlation between PM concentrations and aerosol optical depth in eastern China. Atmospheric Environment, 43(37), pp.5876-5886.
Guo, S., Hu, M., Zamora, M.L., Peng, J., Shang, D., Zheng, J., Du, Z., Wu, Z., Shao, M., Zeng, L. and Molina, M.J.: Elucidating severe urban haze formation in China. P. Natl. Acad. Sci., 111, 17,373–17,378. https://doi.org/10.1073/pnas.1419604111, 2014.Geiß, A., Wiegner, M., Bonn, B., Schäfer, K., Forkel, R., Schneidemesser, E.V., Münkel, C., Chan, K.L. and Nothard, R.: Mixing layer height as an indicator for urban air quality?. Atmospheric Measurement Techniques, 10(8), pp.2969-2988, 2017.
Rienecker, M.M., et al., 2011. MERRA: NASA's Modern-Era retrospective analysis for research and applications. J. Clim. 24, 3624e3648. http://dx.doi.org/10.1175/ JCLI-D-11-00015.1.
Hägeli, P., Steyn, D. and Strawbridge, K.: Spatial and temporal variability of mixed-layer depth and entrainment zone thickness. Boundary Layer Meteorol., 97(1), 47–71. https://doi.org/10.1023/A:1002790424133, 2000.
He, Q., Li, C., Mao, J., Lau, A. K.-H., and Chu, D. A.: Analysis of aerosol vertical distribution and variability in Hong Kong. J. Geophys. Res., 113, D14211. https://doi.org/10.1029/2008JD009778, 2008.
Hooper, W. P. and Eloranta, E. W.: Lidar measurements of wind in the planetary boundary layer – the method, accuracy and results from joint measurements with radiosonde and kytoon. Boundary Layer Meteorol., 25(7), 1986.
Huang, R.J., Zhang, Y., Bozzetti, C., Ho, K.F., Cao, J.J., Han, Y., Daellenbach, K.R., Slowik, J.G., Platt, S.M., Canonaco, F. and Zotter, P.: High secondary aerosol contribution to particulate pollution during haze events in China. Nature, 514(7521), 218.
Huang, X., Wang, Z. and Ding, A.: Impact of Aerosol‐PBL Interaction on Haze Pollution: Multi‐Year Observational Evidences in North China. Geophysical Research Letters, 2018.
Jacob, DJ. Heterogeneous chemistry and tropospheric ozone. Atmos Environ 2000; 34(12): 2131-2159, 2014.
Johnson, R. H., Ciesielski, P. E., and Cotturone, J. A.: Multiscale variability of the atmospheric mixed layer over the western Pacific warm pool. Journal of the Atmospheric Sciences, 58, 2,729–2,750, 2001.
Jordan, N. S., R. M. Hoff., and J. T. Bacmeister.: Validation of Goddard Earth Observing System-version 5 MERRA planetary boundary layer heights using CALIPSO, J. Geophys. Res., 115, D24218, doi:10.1029/2009JD013777, 2010.
Kiehl, J. T. and Briegleb, B. P.: The relative roles of sulfate aerosols and greenhouse gases in climate forcing. Science, 260, 311–314. https://doi.org/10.1126/science.260.5106.311, 1993.
Kendall, M. G. (1975), Rank Correlation Methods, pp. 1–202, Griffin, London.
Knote, C., Tuccella, P., Curci, G., Emmons, L., Orlando, J.J., Madronich, S., Baró, R., Jiménez-Guerrero, P., Luecken, D., Hogrefe, C., Forkel, R., Werhahne, J., Hirtl, M., Pérez, J., José,

R., Giordano, L., Brunner, D., Yahya, K., Zhang, Y.: Influence of the choice of gas-phase mechanism on predictions of key gaseous pollutants during the AQMEII phase-2 intercomparison. Atmos. Environ., 115, 553–568. https://doi.org/10.1016/j.atmosenv.2014.11.066, 2015.

Kennedy, A.D., Dong, X., Xi, B., Xie, S., Zhang, Y., Chen, J., 2011. A comparison of MERRA and NARR reanalyses with the DOE ARM SGP data. J. Clim. 24 (17), 4541e4557.

L'Ecuyer, T. S. and Jiang, J. H.: Touring the atmosphere aboard the A-Train. Physics Today, 63(7), 36–41, 2010.

LeMone, M. A., Tewari, M., Chen, F., and Dudhia, J.: Objectively determined fair-weather CBL depths in the ARW-WRF model and their comparison to CASES-97 observations. Monthly Weather Review, 141, 30–54. https://doi.org/10.1175/MWR-D-12- 00106.1, 2013

Leventidou, E., Zanis, P., Balis, D., Giannakaki, E., Pytharoulis, I., and Amiridis, V.: Factors affecting the comparisons of planetary boundary layer height retrievals from CALIPSO, ECMWF and radiosondes over Thessaloniki, Greece. Atmos. Environ., 74, 360–366. https://doi.org/10.1016/j.atmosenv.2013.04.007, 2013.

Levy, R.C., Remer, L.A., Kleidman, R.G., Mattoo, S., Ichoku, C., Kahn, R., and Eck, T.F.: Global evaluation of the Collection 5 MODIS dark-target aerosol products over land. Atmos. Chem. Phys. 10 (21), 10399e10420, 2010.

Li, J., Li, C., Zhao, C. and Su, T.: Changes in surface aerosol extinction trends over China during 1980 - 2013 inferred from quality - controlled visibility data. Geophys. Res. Lett., 43(16), pp.8713-8719, 2016.

Li, J., Wang, Z., Wang, X., Yamaji, K., Takigawa, M., Kanaya, Y., Pochanart, P., Liu, Y., Irie, H., Hu, B., Tanimoto, H., and H. Akimoto.: Impacts of aerosols on summertime tropospheric photolysis frequencies and photochemistry over Central Eastern China. Atmos. Environ., 45(10), 1,817–1,829. https://doi.org/10.1016/j.atmosenv.2011.01.016, 2011.

Li, Z., Guo, J., Ding, A., Liao, H., Liu, J., Sun, Y., and Zhu, B.: Aerosol and boundary-layer interactions and impact on air quality. National Science Review, nwx117. https://doi.org/10.1093/nsr/nwx117, 2017.

Li, Z., Lau, W.M., Ramanathan, V., Wu, G., Ding, Y., Manoj, M.G., Liu, J., Qian, Y., Li, J., Zhou, T. Fan, J., D. Rosenfeld., Y. Ming., Y. Wang., J. Huang., B. Wang., X. Xu., S.-S. Lee., M. Cribb., F. Zhang., X. Yang., C. Zhao., T. Takemura., K. Wang., X. Xia., Y. Yin., H. Zhang., J. Guo., P. M. Zhai., N. Sugimoto., S. S. Babu., and G. P. Brasseur.: Aerosol and monsoon climate interactions over Asia. Reviews of Geophysics, 54, 866–929. https://doi.org/10.1002/2015RG000500, 2016.

Li, Z., Rosenfeld, D., and Fan, J.: Aerosols and their Impact on Radiation, Clouds, Precipitation and Severe Weather Events, Oxford Encyclopedia in Environmental Sciences, 10.1093/acrefore/9780199389414.013.126, 2017a.

Lin, C.Q., Li, C.C., Lau, A.K., Yuan, Z.B., Lu, X.C., Tse, K.T., Fung, J.C., Li, Y., Yao, T., Su, L. and Li, Z.Y.: Assessment of satellite-based aerosol optical depth using continuous lidar observation. Atmospheric environment, 140, pp.273-282, 2016.,

Liao, H. and Seinfeld, J. H.: Global impacts of gas - phase chemistry - aerosol interactions on direct radiative forcing by anthropogenic aerosols and ozone. J. Geophys. Res., 110(D18), 2005.

Liu, J., Huang, J., Chen, B., Zhou, T., Yan, H., Jin, H., Huang, Z. and Zhang, B.: Comparisons of PBL heights derived from CALIPSO and ECMWF reanalysis data over China. Journal of Quantitative Spectroscopy and Radiative Transfer, 153, 102–112. https://doi.org/10.1016/j.jqsrt.2014.10.011,

2015.
Liang, X., S. Li, S. Y. Zhang, H. Huang, and S. X. Chen (2016), PM2.5 data reliability, consistency, and air quality assessment in five Chinese cities, J Geophys Res-Atmos, 121(17), 10220-10236.
Liu, S. and Liang, X.-Z.: Observed diurnal cycle climatology of planetary boundary layer height. Journal of Climate, 22(21), 5,790–5,809. https://doi.org/10.1175/ 2010JCLI3552.1, 2010.
McGrath-Spangler, E. L. and Denning, A. S.: Estimates of North American summertime planetary boundary layer depths derived from space-borne lidars. J. Geophys. Res., 117. https://doi.org/10.1029/012JD017615, 2012.
Melfi, S. H., Whiteman, D., and Ferrare, R.: Observation of atmospheric fronts using Raman lidar moisture measurements. Journal of Applied Meteorology, 28(9), 789–806. https://doi.org/10.1175/1520-0450(1989)028<0789:OOAFUR>2.0.CO;2, 1989.
Miao, Y., Guo, J., Liu, S., Liu, H., Li, Z., Zhang, W. and Zhai, P.: Classification of summertime synoptic patterns in Beijing and their associations with boundary layer structure affecting aerosol pollution. Atmos. Chem. Phys., 17, 3,097–3,110. https://doi.org/10.5194/acp-17-3097-2017, 2017.
Miao, Y., Liu, S., Zheng, Y., and Wang, S.: Modeling the feedback between aerosol and boundary layer processes: a case study in Beijing, China. Environmental Science and Pollution Research, 23(4), 3,342–3,357. https://doi.org/10.1007/s11356-015-5562-8, 2016.
Mann, H. B. (1945), Nonparametric tests against trend, Econometrica, 13, 245–259.
Mok, J., Krotkov, N.A., Arola, A., Torres, O., Jethva, H., Andrade, M., Labow, G., Eck, T.F., Li, Z., Dickerson, R.R., Stenchikov, G.L., Sergey Osipov., and Xinrong Ren.: Impacts of brown carbon from biomass burning on surface UV and ozone photochemistry in the Amazon Basin, Scientific Report, DOI: 10.1038/srep36940, 2016.
Petäjä, T., Järvi, L., Kerminen, V.M., Ding, A.J., Sun, J.N., Nie, W., Kujansuu, J., Virkkula, A., Yang, X., Fu, C.B., Zilitinkevich, S., and M. Kulmala.: Enhanced air pollution via aerosol-boundary layer feedback in China. Scientific Reports, 6. https://doi.org/10.1038/srep18998, 2016.
Qu, Y., Han, Y., Wu, Y., Gao, P., and Wang, T.: Study of PBLH and Its Correlation with Particulate Matter from One-Year Observation over Nanjing, Southeast China. Remote Sensing, 9(7), p.668, 2017.
Ravishankara, AR. Heterogeneous and multiphase chemistry in the troposphere. Science, 276(5315): 1058-1065, 1997.
Sawyer, V. and Li, Z.: Detection, variations and intercomparison of the planetary boundary layer depth from radiosonde, lidar and infrared spectrometer. Atmos. Environ., 79, 518–528. https://doi.org/10.1016/j.atmosenv.2013.07.019, 2013.
Schafer, J.S., Eck, T.F., Holben, B.N., Thornhill, K.L., Anderson, B.E., Sinyuk, A., Giles, D.M., Winstead, E.L., Ziemba, L.D., Beyersdorf, A.J. and Kenny, P.R.: Intercomparison of aerosol single - scattering albedo derived from AERONET surface radiometers and LARGE in situ aircraft profiles during the 2011 DRAGON - MD and DISCOVER - AQ experiments. J. Geophys. Res., 119(12), 7439-7452, 2014. Scott, D.W., 2015. Multivariate density estimation: theory, practice, and visualization. John Wiley & Sons.
Simmons, A., ERA-Interim: New ECMWF reanalysis products from 1989 onwards, ECMWF newsletter, 110, 25-36., 2006.
Seibert, P., Beyrich, F., Gryning, S.-E., Joffre, S., Rasmussen, A., and Tercier, P.: Review and intercomparison of operational methods for the determination of the mixing height. Atmos.

Formatted: Font: 10 pt

Formatted: Indent: Left: 0 cm, Hanging: 0.92 cm, First line: 0 ch, Line spacing: 1.5 lines

Formatted

Formatted: Font: Times New Roman

Environ.t, 34(7), 1,001–1,027. https://doi.org/10.1016/S1352-2310(99)00349-0, 2000.
Su, T., Li, J., Li, C., Lau, A. K. H., Yang, D., and Shen, C.: An intercomparison of AOD-converted PM2.5 concentrations using different approaches for estimating aerosol vertical distribution. Atmos. Environ., 166, 531-542, 2017a.
Su, T., Li, J., Li, C., Xiang, P., Lau, A.K.H., Guo, J., Yang, D., and Miao, Y.: An intercomparison of long-term planetary boundary layer heights retrieved from CALIPSO, ground-based lidar, and radiosonde measurements over Hong Kong. J. Geophys. Res., 122(7), pp.3929-3943, 2017b.
Tang, G., Zhang, J., Zhu, X., Song, T., Münkel, C., Hu, B., Schäfer, K., Liu, Z., Zhang, J., Wang, L., Xin, J., Suppan, P., and Wang, Y.: Mixing layer height and its implications for air pollution over Beijing, China. Atmos. Chem. Phys., 16, 2,459–2,475. https://doi.org/10.5194/acp-16-2459-2016, 2016.
Tie, X., Zhang, Q., He, H., Cao, J., Han, S., Gao, Y., Li, X. and Jia, X.C.: A budget analysis of the formation of haze in Beijing. Atmos. Environ., 100, pp.25-36, 2015.
Tucker, S.C., Senff, C.J., Weickmann, A.M., Brewer, W.A., Banta, R.M., Sandberg, S.P., Law, D.C. and Hardesty, R.M.: Doppler lidar estimation of mixing height using turbulence, shear, and aerosol profiles. J. Atmos. Oceanic Technol., 26(4), 673–688. https://doi.org/10.1175/2008JTECHA1157.1, 2009.
Vogelezang, D. H. P. and Holtslag, A. A. M.: Evaluation and model impacts of alternative boundary layer height formulations. Boundary Layer Meteorol., 81(3-4), 245–269. https://doi.org/10.1007/BF02430331, 1996.
Wang, G., Zhang, R., Gomez, M. E., Yang, L., Zamora, M. L., Hu, M., Lin, Y., Peng, J., Guo, S., and Meng, J.: Persistent sulfate formation from London Fog to Chinese haze, P. Natl. Acad. Sci., 113, 13630–13635, 2016.
Wang, X., Dickinson, R. E., Su, L., Zhou, C., and Wang, K.: PM2.5 pollution in China and how it has been exacerbated by terrain and meteorological conditions. Bulletin of the American Meteorological Society. https://doi.org/10.1175/BAMS-D-16-0301.1, 2017.
Wang, Y., Khalizov, A., and Zhang, R.: New directions: light-absorbing aerosols and their atmospheric impacts. Atmos. Environ., 81, 713–715. https://doi.org/10.1016/j.atmosenv.2013.09.034, 2013.
Winker, D. M., Hunt, W. H., and McGill, M. J.: Initial performance assessment of CALIOP. Geophys. Res. Lett., 34, L19803. https://doi.org/10.1029/ 2007GL030135, 2007.
Winker, D.M., Vaughan, M.A., Omar, A., Hu, Y., Powell, K.A., Liu, Z., Hunt, W.H. and Young, S.A.: Overview of the CALIPSO mission and CALIOP data processing algorithms. J. Atmos. Oceanic Technol., 26, 2,310–2,323. https://doi.org/10.1175/2009JTECHA1281.1, 2009.
Winship, C. and Radbill, L., 1994. Sampling weights and regression analysis. Sociological Methods & Research, 23(2), pp.230-257.
Yang, D., Li, C., Lau, A. K. H., and Li, Y.: Long-term measurement of daytime atmospheric mixing layer height over Hong Kong. J. Geophys. Res., 118, 2,422–2,433. https://doi.org/10.1002/jgrd.50251, 2013.
Zhang, W., Guo, J., Miao, Y., Liu, H., Zhang, Y., Li, Z., and Zhai, P.: Planetary boundary layer height from CALIOP compared to radiosonde over China. Atmos. Chem. Phys., 16, 9,951–9,963. https://doi.org/10.5194/acp-16-9951-2016., 2016..

Formatted: Indent: Left: 0 cm, Hanging: 2 ch, First line: -2 ch, Line spacing: single, No page break before

Table 1. Description of datas.

Observations	Variables	Location	Temporal resolution	Time period
Environmental Stations	$PM_{2.5}$	~1600 sites*	Hourly	01/201201-06/201706
Meteorological Stations	WS/WD	~900 sites**	Hourly	01/201201-06/201706
MPL	PBLH, extinction	Beijing	15seconds	043/201604-12/201712
AERONET	AOD (550nm),	Beijing	~Hourly	01/201601-12/201712
MODIS	AOD	Whole China	Daily	01/200601-12/201712
CALIPSO	PBLH	Orbits in Figure 1d	Daily	06/200606-12/201712
MERRA	PBLH	Whole China	Hourly	01/200601-12/201712

* 224 sites over NCP; 105 sites over PRD; 215 sites over YRD; 159 sites over NEC

** 37 sites over NCP; 92 sites over PRD; 34 sites over YRD; 76 sites over NEC

Mean values and standard deviation (STD) of CALIPSO-PBLH, MERRA-PBLH, and $PM_{2.5}$ over different ROIs.

Parameter			NCP	PRD	YRD	NEC
CALIPSO-PBLH (km)	MAM	Mean	1.40	1.35	1.31	1.40
		STD	0.54	0.47	0.48	0.59
	JJA	Mean	1.47	1.27	1.24	1.46
		STD	0.51	0.44	0.46	0.55
	SON	Mean	1.21	1.24	1.26	1.15
		STD	0.45	0.36	0.39	0.50
	DJF	Mean	1.06	1.07	1.12	0.94
		STD	0.40	0.34	0.41	0.47
MERRA-PBLH (km)	MAM	Mean	1.57	1.16	1.24	1.45
		STD	0.75	0.53	0.47	0.69
	JJA	Mean	1.46	0.99	1.07	1.49
		STD	0.72	0.36	0.39	0.68
	SON	Mean	1.37	1.18	1.22	1.19

Formatted Table

Formatted: No page break before

Formatted: Font: 9.5 pt

		STD	0.48	0.37	0.33	0.54
	DJF	Mean	1.08	1.09	1.05	0.65
		STD	0.36	0.40	0.32	0.36
PM$_{2.5}$ ($\mu g \cdot m^{-3}$)	MAM	Mean	63.1	32.8	50.4	34.8
		STD	45.1	22.1	29.2	29.4
	JJA	Mean	51.2	25.1	37.9	29.6
		STD	36.8	20.4	24.1	24.4
	SON	Mean	70.9	39.3	42.4	44.2
		STD	58.4	23.1	28.3	49.1
	DJF	Mean	102.7	44.2	69.8	60.3
		STD	84.2	28.3	51.3	54.4

906

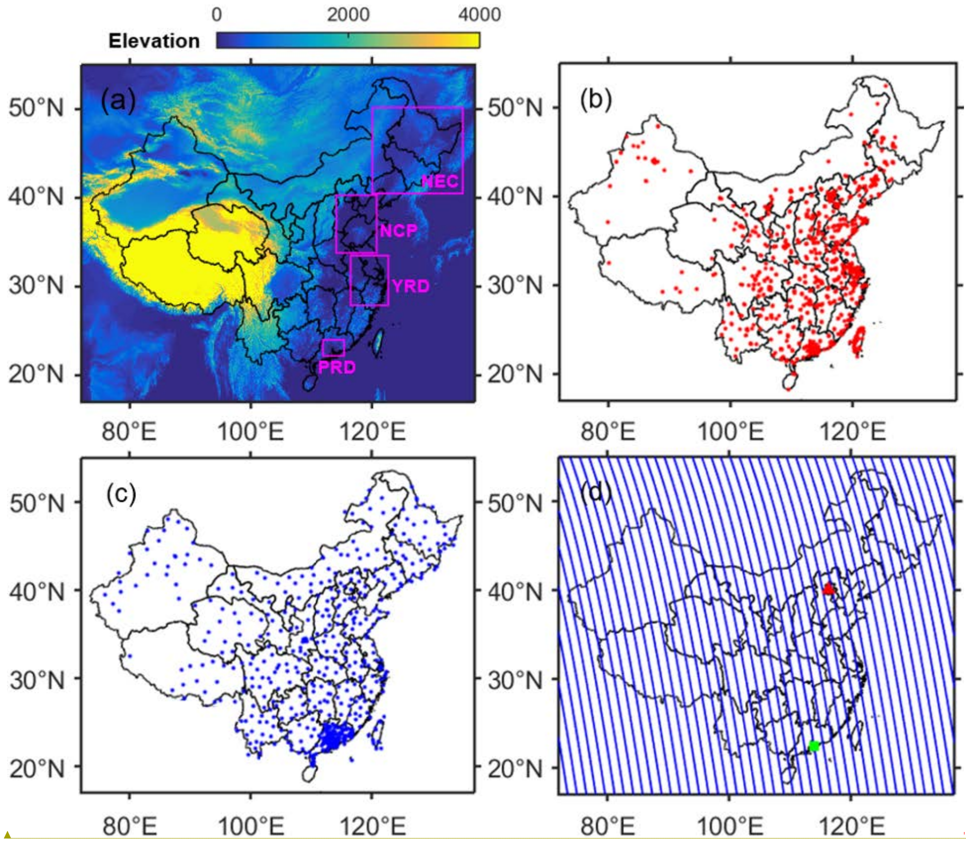

Formatted: Font: 10 pt, Bold

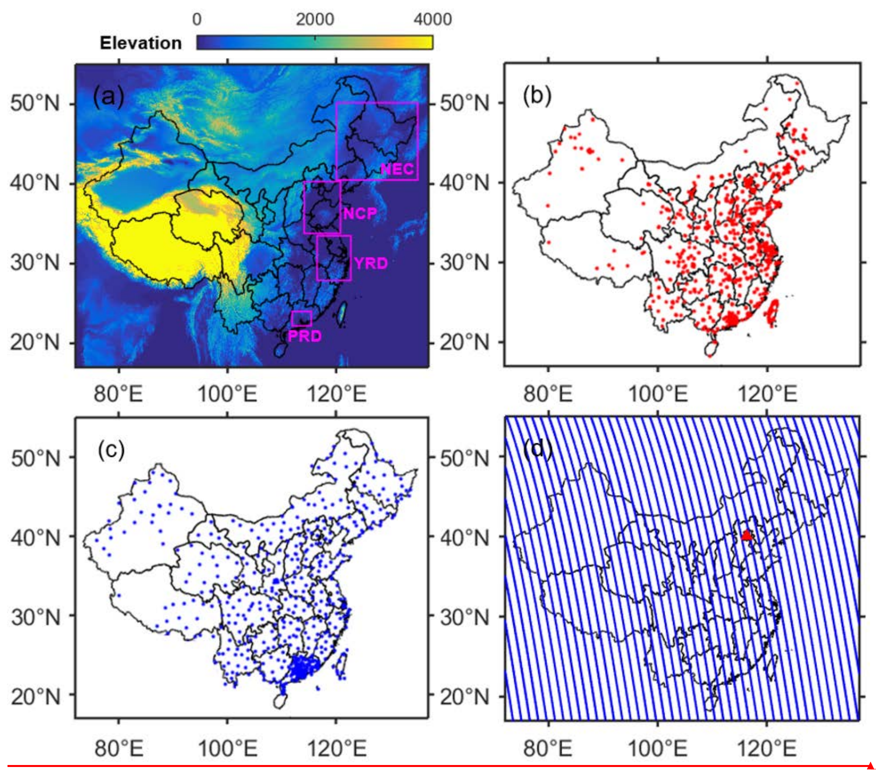

Figure 1. (a) Topography of China. The black rectangles outline the five regions of interest: northeast China (NEC): 40.5-50.2°N, 120.1-135°E; North China Plain (NCP): 33.8-40.3°N, 114.1-120.8°E; Pearl River Delta (PRD): 22.2-24°N, 111.9-115.4°E; and Yangtze River Delta (YRD): 27.9-33.5°N, 116.5-122.7°E. Locations of (b) environmental stations and (c) meteorological stations. (d) Blue lines indicate CALIOP daytime orbits (in ascending node). Ground-based lidar and sun-photometer are deployed at Beijing (red triangle~~circle~~)~~, and sun-photometer is deployed at Hong Kong (green circle)~~.

Formatted: Font: Bold

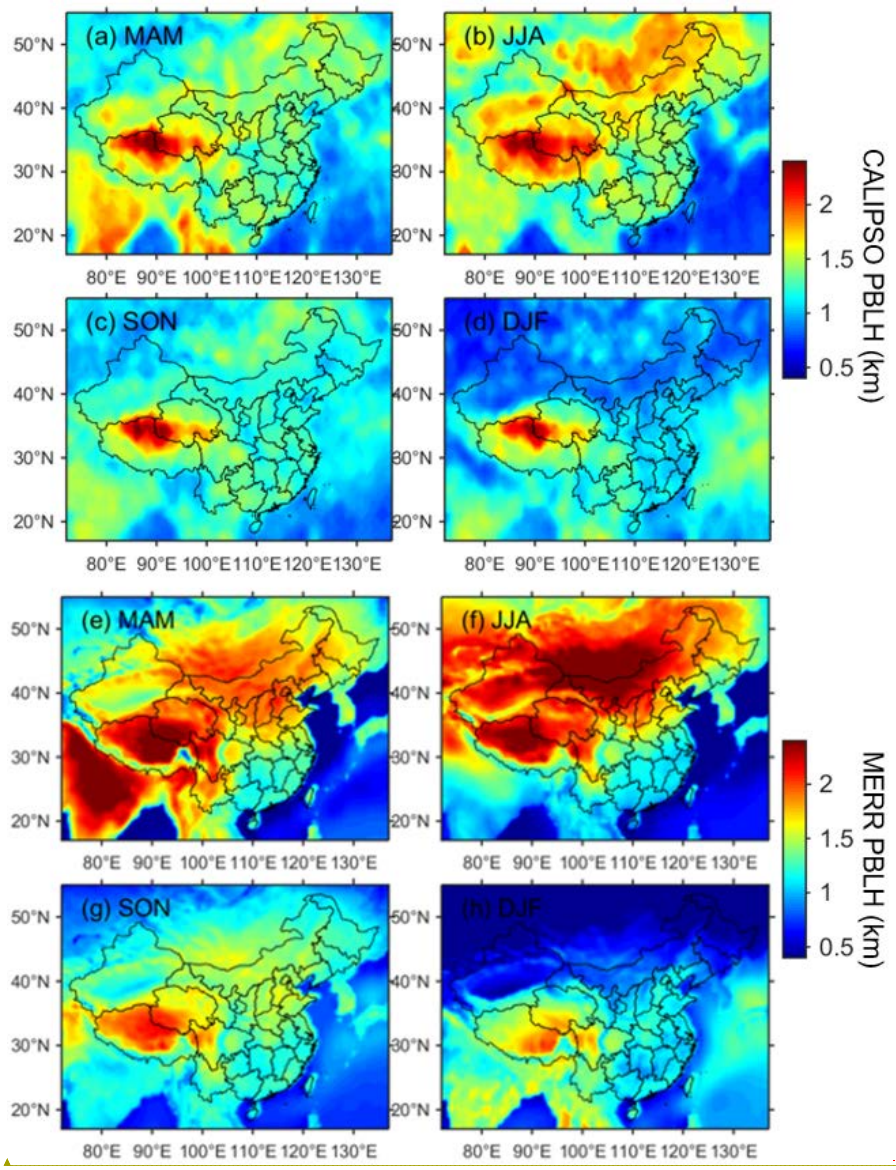

Formatted: Font: 10 pt

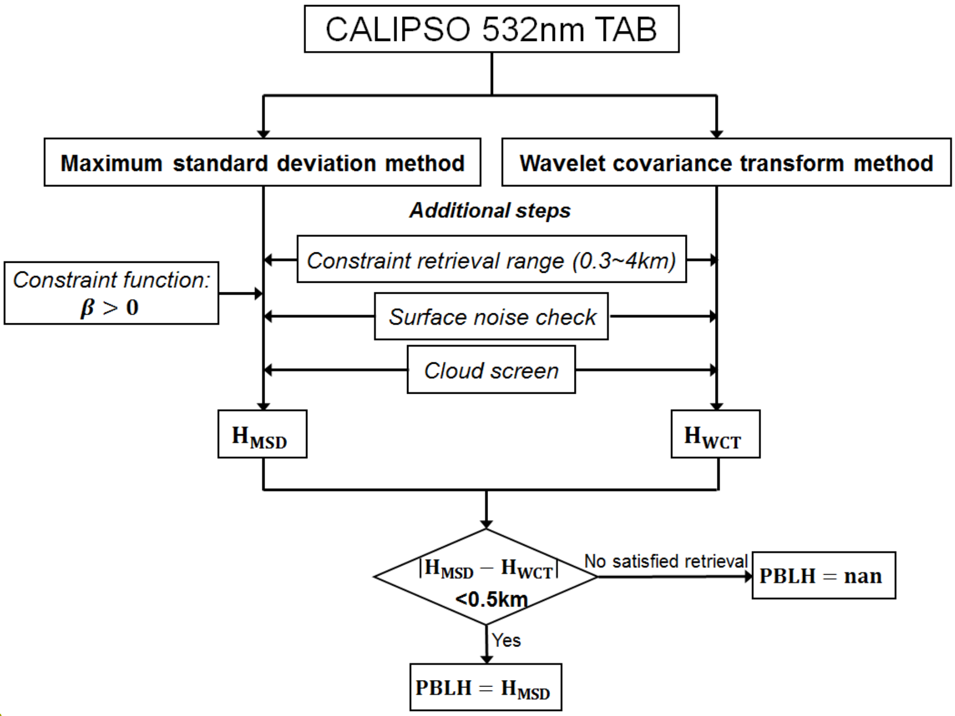

Figure 2. The schematic diagram of retrieving the PBLH from CALIPSO.

Formatted: Font: 10 pt

Formatted: Font: 10 pt

Formatted: Font: 10 pt

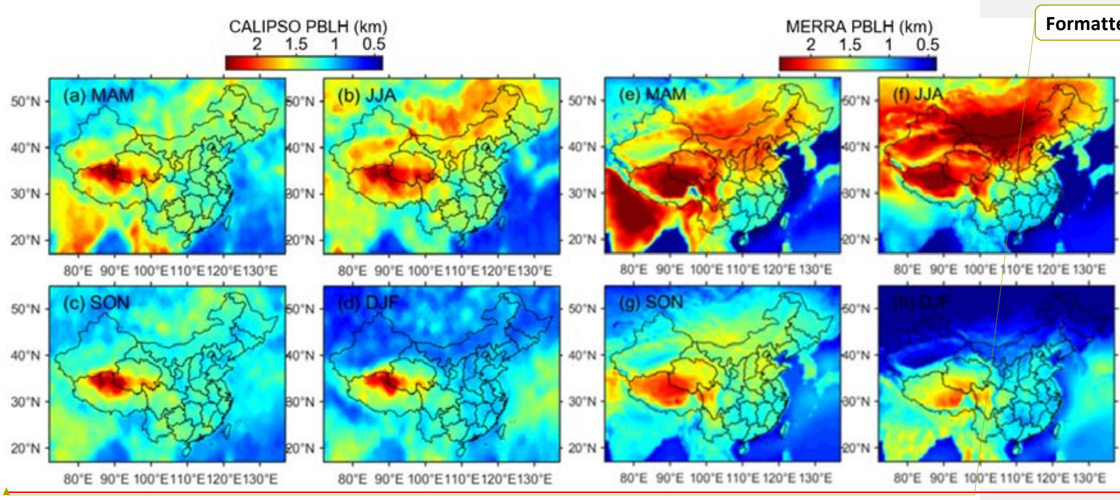

Formatted: Font: 10 pt

Figure ~~2~~3. Spatial distributions of climatological mean PBLH derived from CALIPSO for (a) March-April-May (MAM), (b) June-July-August (JJA), (c) September-October-November (SON), and (d) December-January-February (DJF) during the period 2006–2017. Spatial distributions of climatological mean of early-afternoon ~~noontime~~ PBLH obtained from MERRA for (e) MAM, (f) JJA, (g) SON, and (h) DJF during the same period.

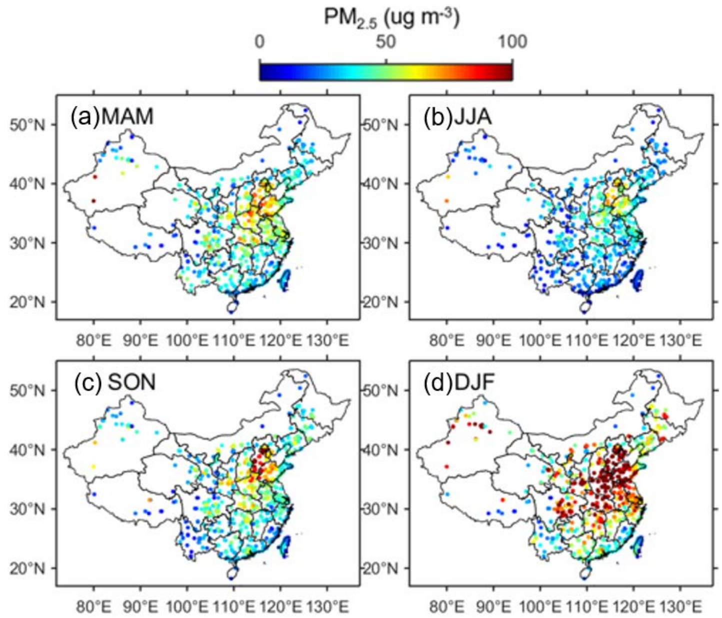

Figure 4. Spatial distributions of climatological mean of early-afternoon $PM_{2.5}$ concentration (in μg m^{-3}) for (a) MAM, (b) JJA, (c) SON, and (d) DJF during the period 2012–2017.

Formatted: Font: 10 pt

Formatted: Centered

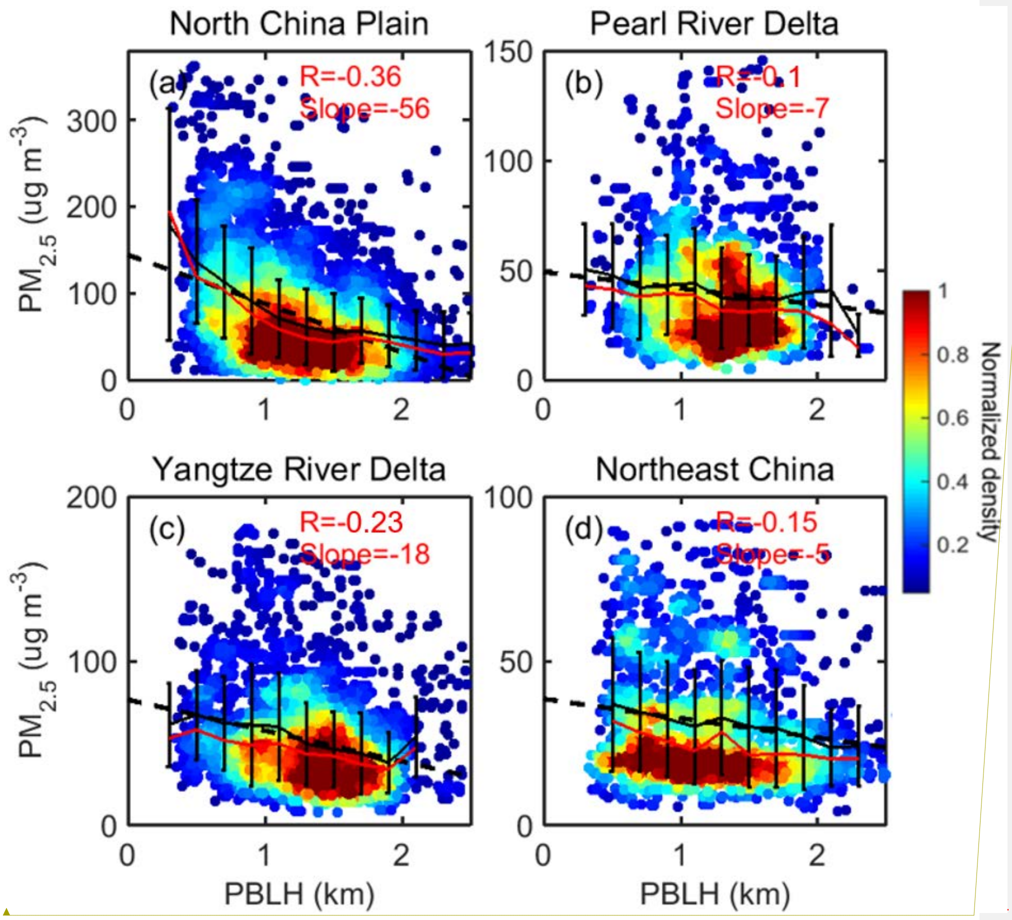

Formatted: Font: 10 pt

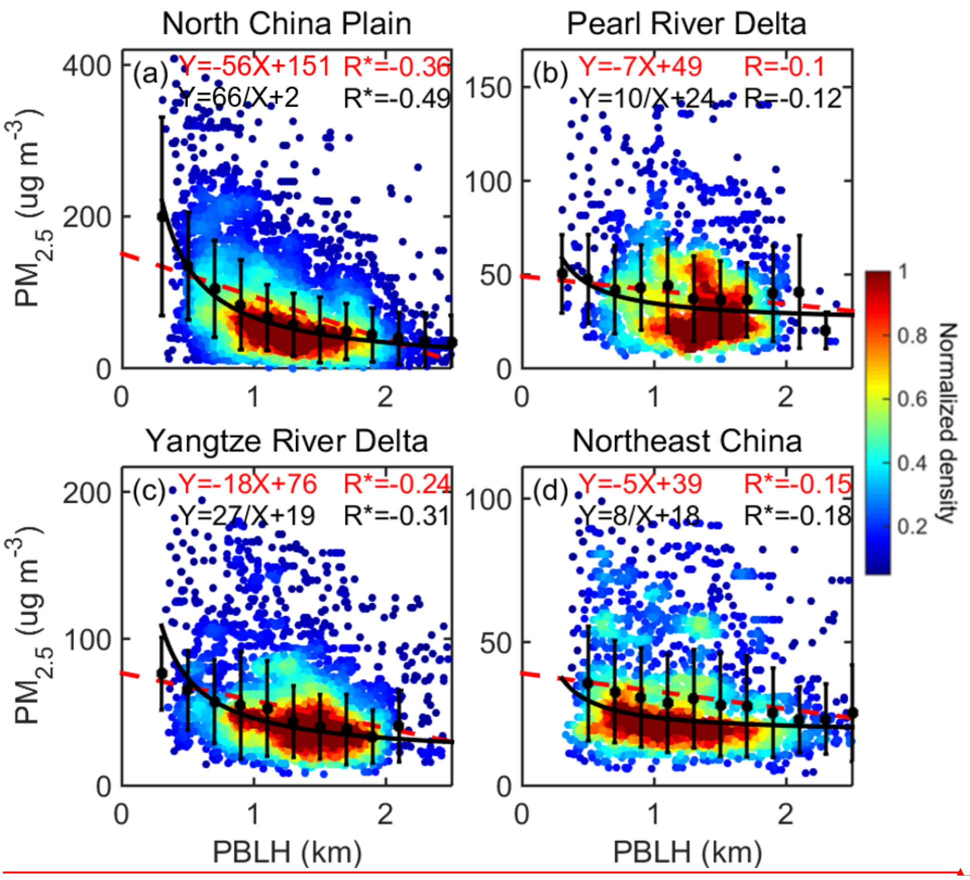

Figure 35. The relationship between CALIPSO-derived PBLH and noontime early-afternoonmid-day $PM_{2.5}$ over (a) NCP, (b) PRD, (c) YRD, and (d) NEC. The black solid linesdots and whiskers represent the average values and standard deviations for each bin., and whiskers indicate one standard deviation. The red solid dash lines highlight indicate the regular median for each binlinear regressions, and the black dashed lines give represent the linear regressionsinverse fit ($f(x) = A/x + B$). The detailed fitting functions are given inat the top of each panels, along with the Pearson correlation coefficient (red) and the correlation coefficient for the inverse fit (black). Here and in the following analysis, R with asterisks indicates the correlations areis statistically significant at the 99% confidence level. The correlation coefficients and slopes for these relationships are shown at the top of each panel. TThe color-shaded dots indicate the normalized sample density.

Formatted: Font: Bold

Comment [ZL18]: Reduce the size of the data points to better see the data density with less overlaps.

Formatted: Font color: Auto

953

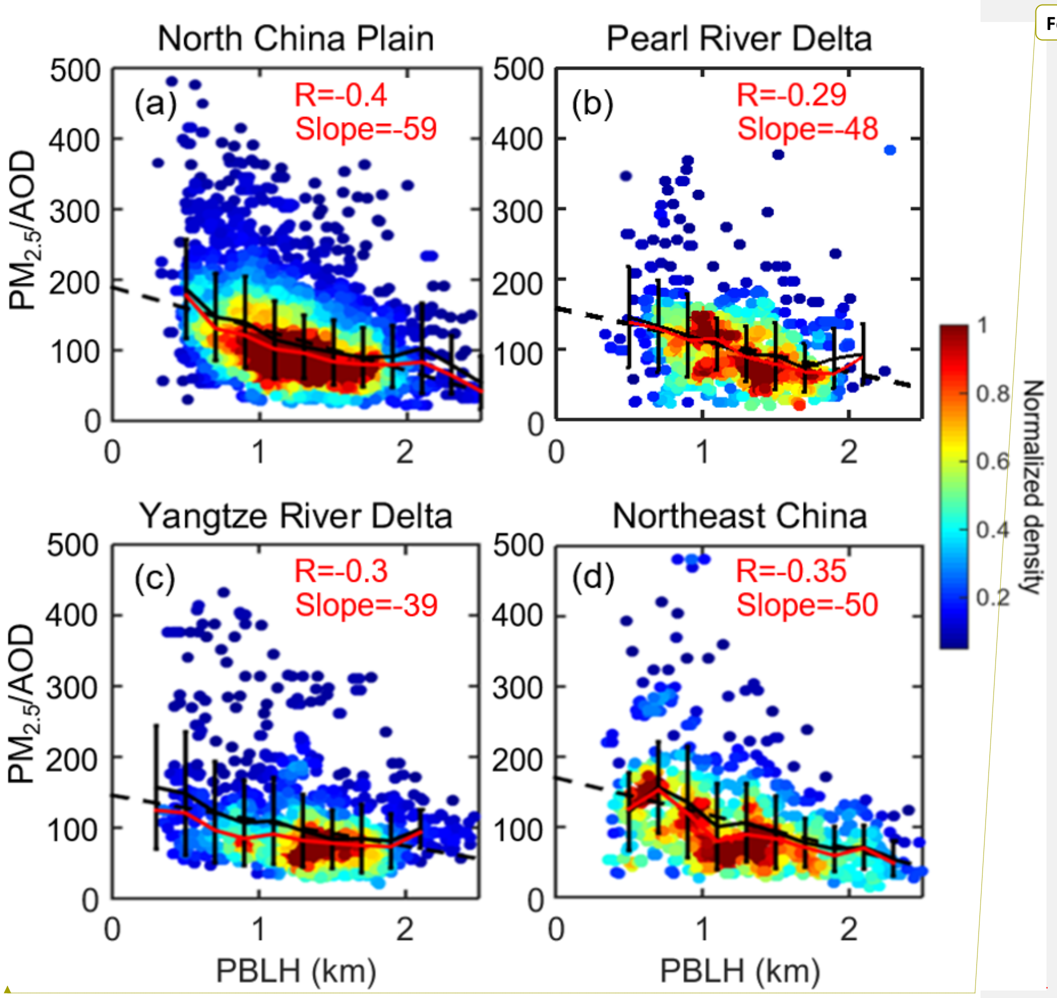

954

955

Formatted: Font: 10 pt

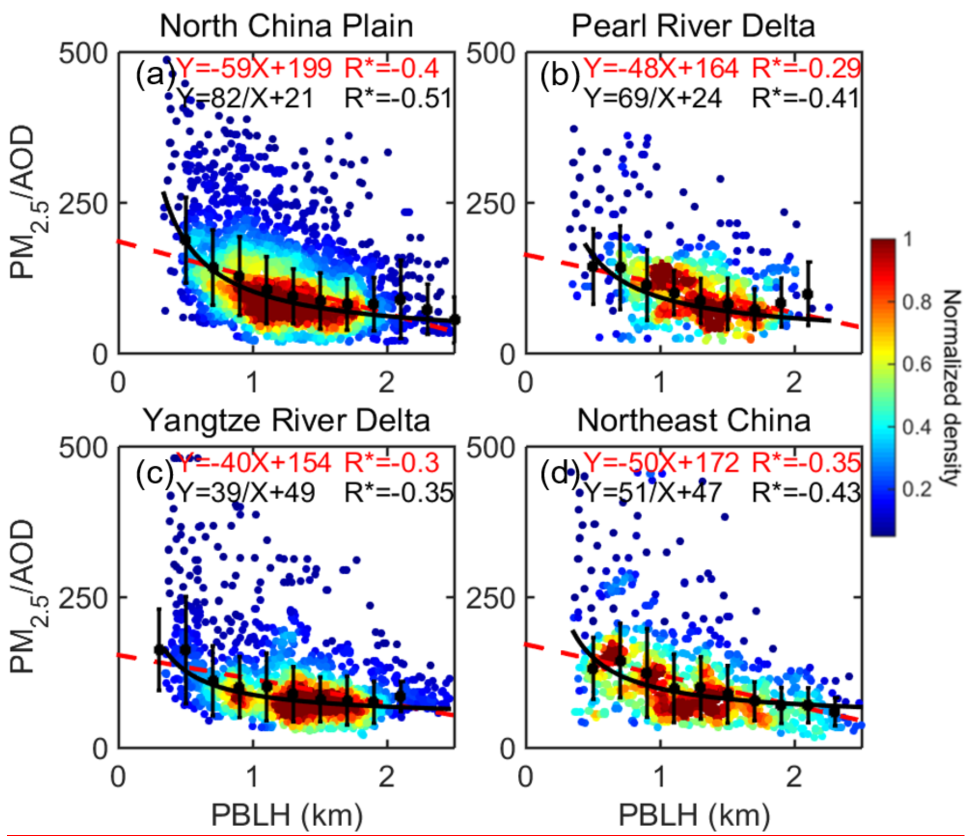

Figure 46. Similar to Figure 35, but for the relationship between CALIPSO PBLH and noontime early-afternoonmid-day $PM_{2.5}$/AOD (unit: μg m^{-3} per AOD) over four ROIs. Here, the AOD data are obtained from MODIS.

Comment [ZL19]: Same as above

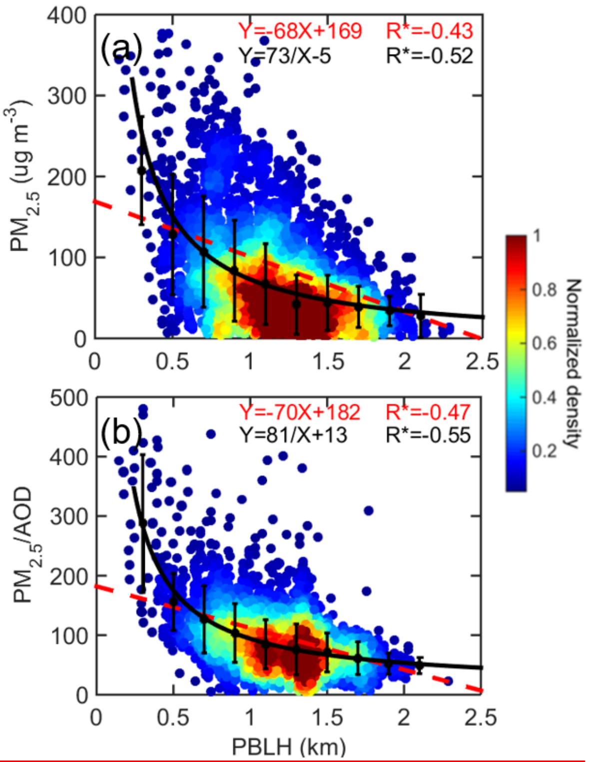

Figure 7. (a) Relationship~~s~~ between MPL-derived PBLH and $PM_{2.5}$ over Beijing. (b) Relationship~~s~~ between MPL-derived PBLH and $PM_{2.5}$/AOD (unit: μg m^{-3} per AOD) over Beijing. ~~Noted T~~the AOD data are obtained from AERONET. Here, linear (red) and inverse fits (black) are both utilized. We use only data acquired during 1000–1500 local time, when the PBL is well developed.

Formatted: Centered

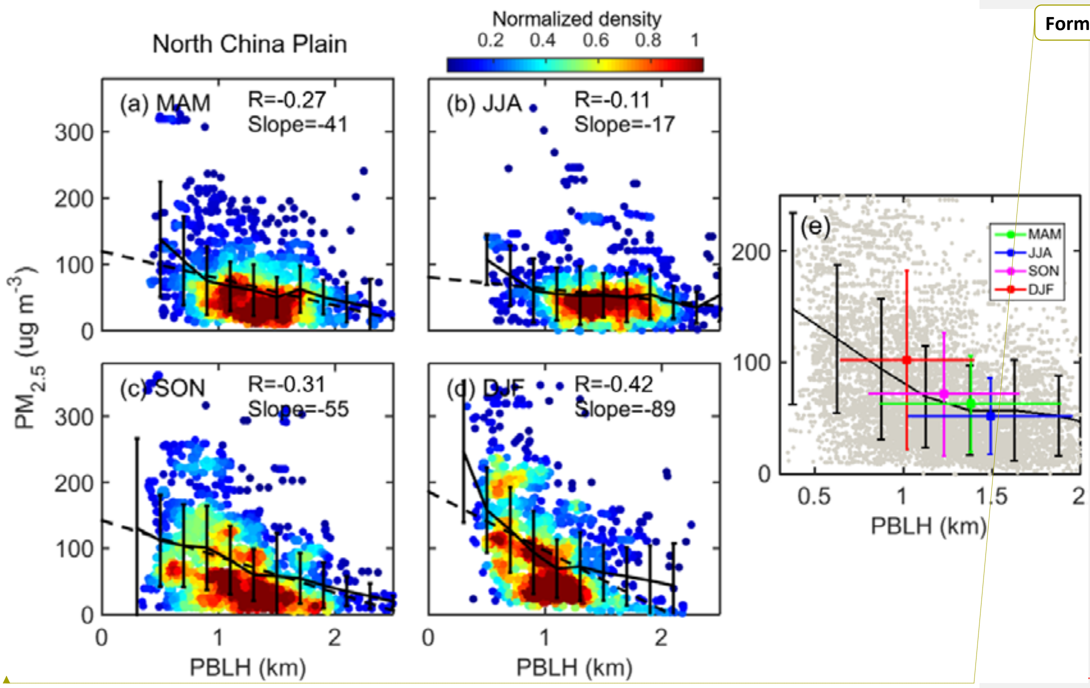

Formatted: Font: 10 pt

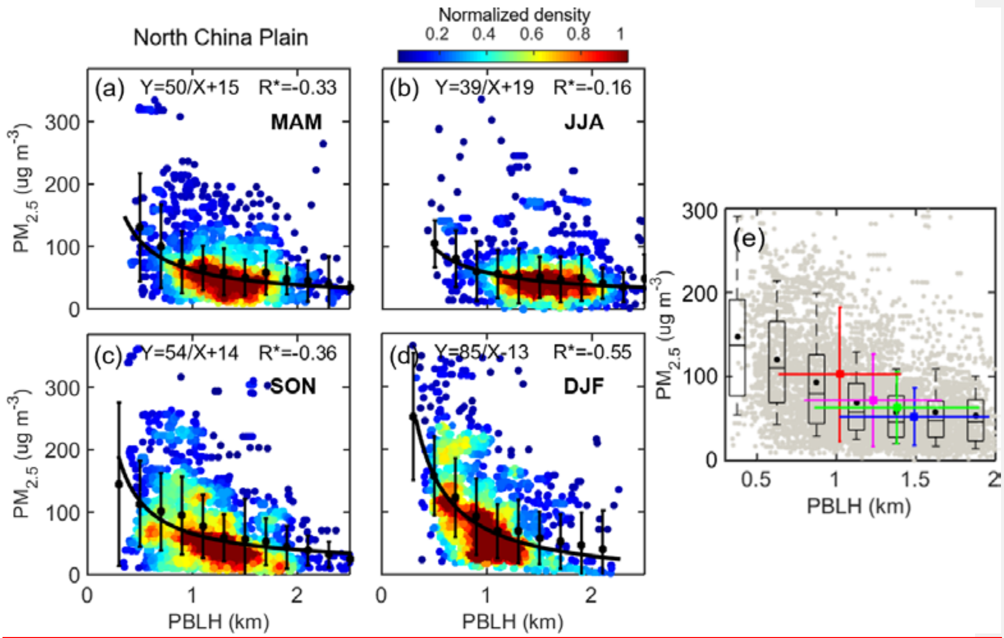

Figure ~~5~~8. The relationship between CALIPSO PBLH and $PM_{2.5}$ over the NCP for (a) MAM, (b) JJA, (c) SON, and (d) DJF. (e) General relationship between $PM_{2.5}$ and PBLH aggregated over all seasons, with individual observations for each day plotted as gray dots. The box-and-whisker plots showing 10th, 25th, 50th, 75th, and 90th percentile values of $PM_{2.5}$ for each bin. –The green, blue, pink, and red dots present the mean values for MAM, JJA, SON, and DJF, respectively. {Please label the vertical axis in Panel e.}

Formatted: Highlight

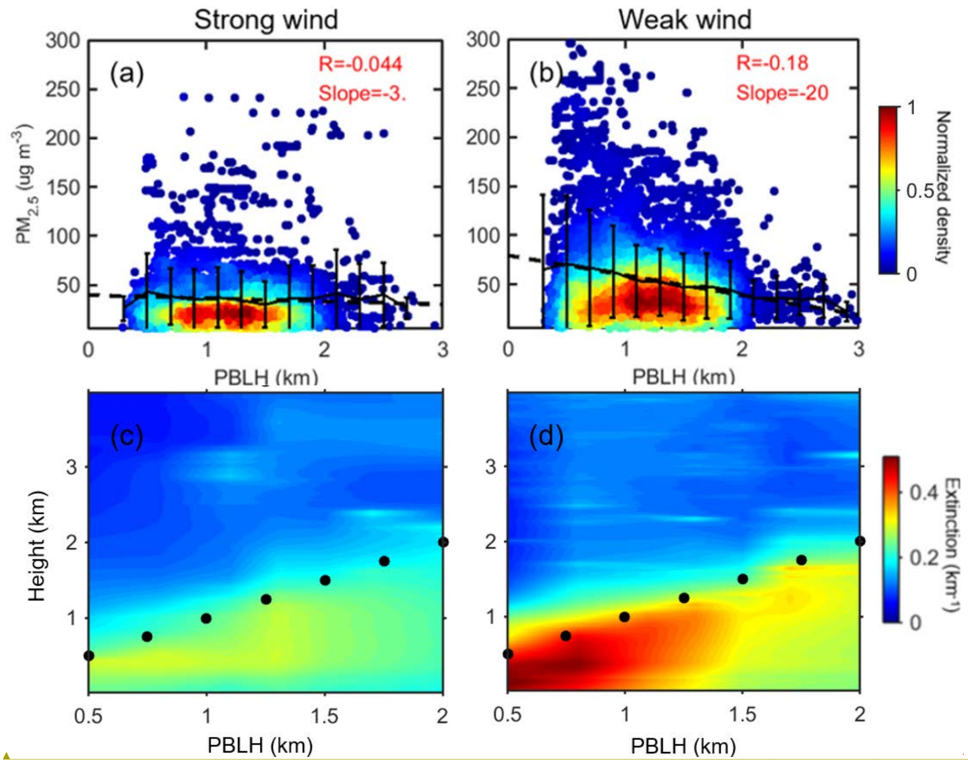

Formatted: Font: 10 pt

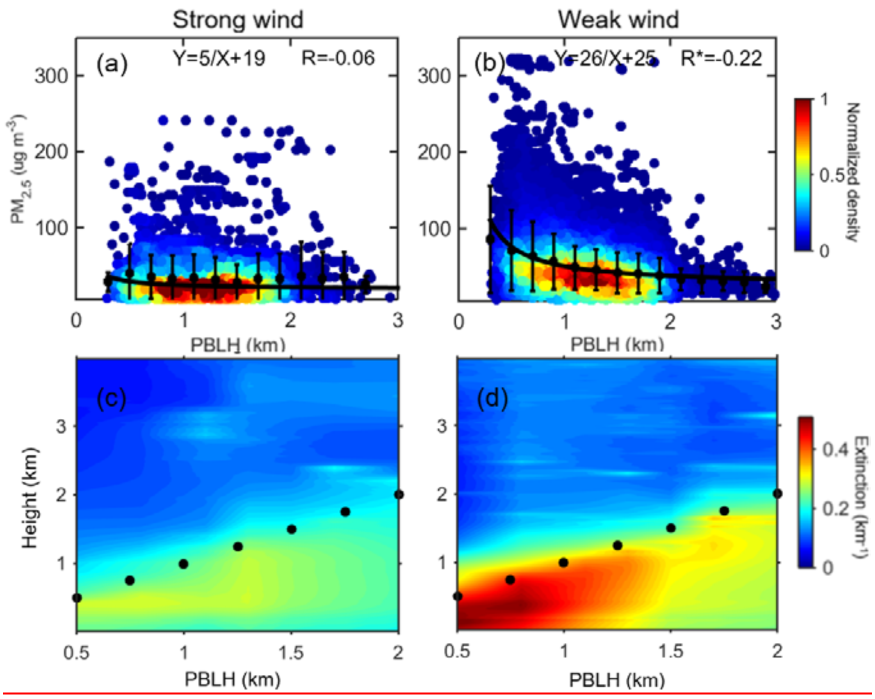

Figure ~~6~~9. The relationship between CALIPSO PBLH and $PM_{2.5}$ over China for (a) strong wind (WS>4m s^{-1}) and (b) weak wind (WS<4m s^{-1}). The aerosol extinction profiles at ~550 nm derived from MPL at Beijing change with different MPL-derived PBLH under (c) strong wind and (d) weak wind conditions. In (c, d), the black dots indicate the location of PBL top.

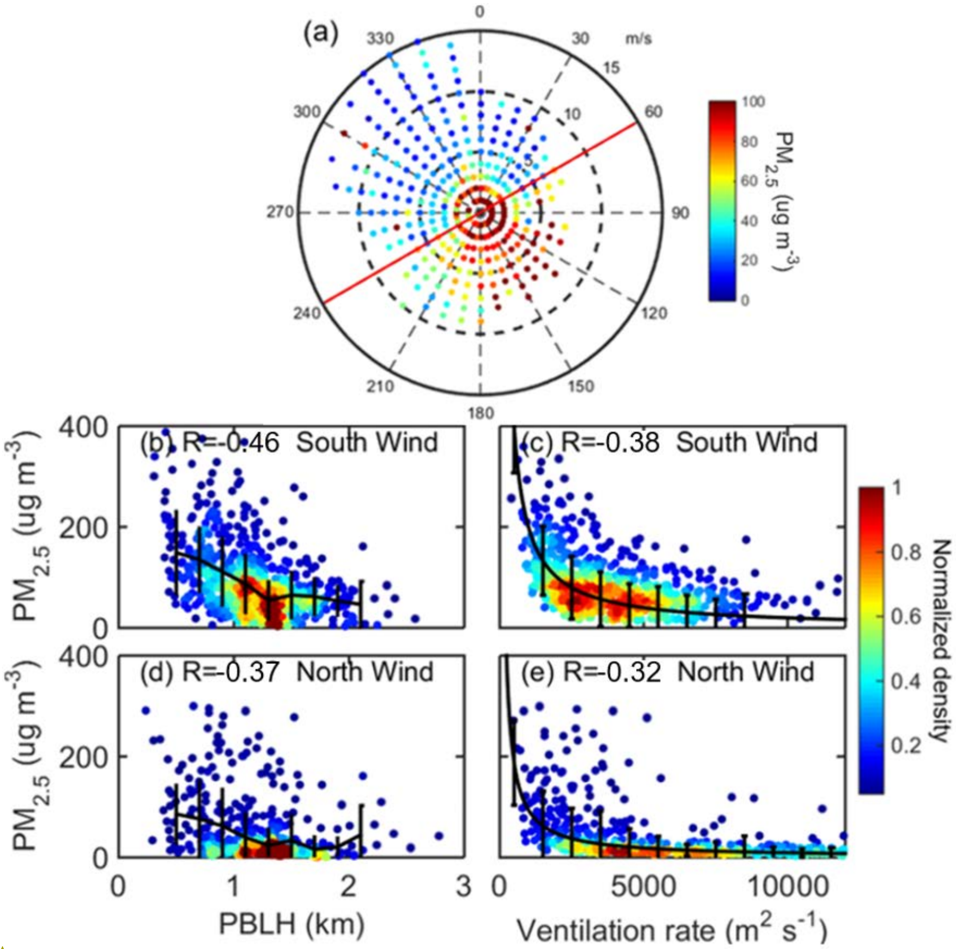

992

Formatted: Font: 10 pt

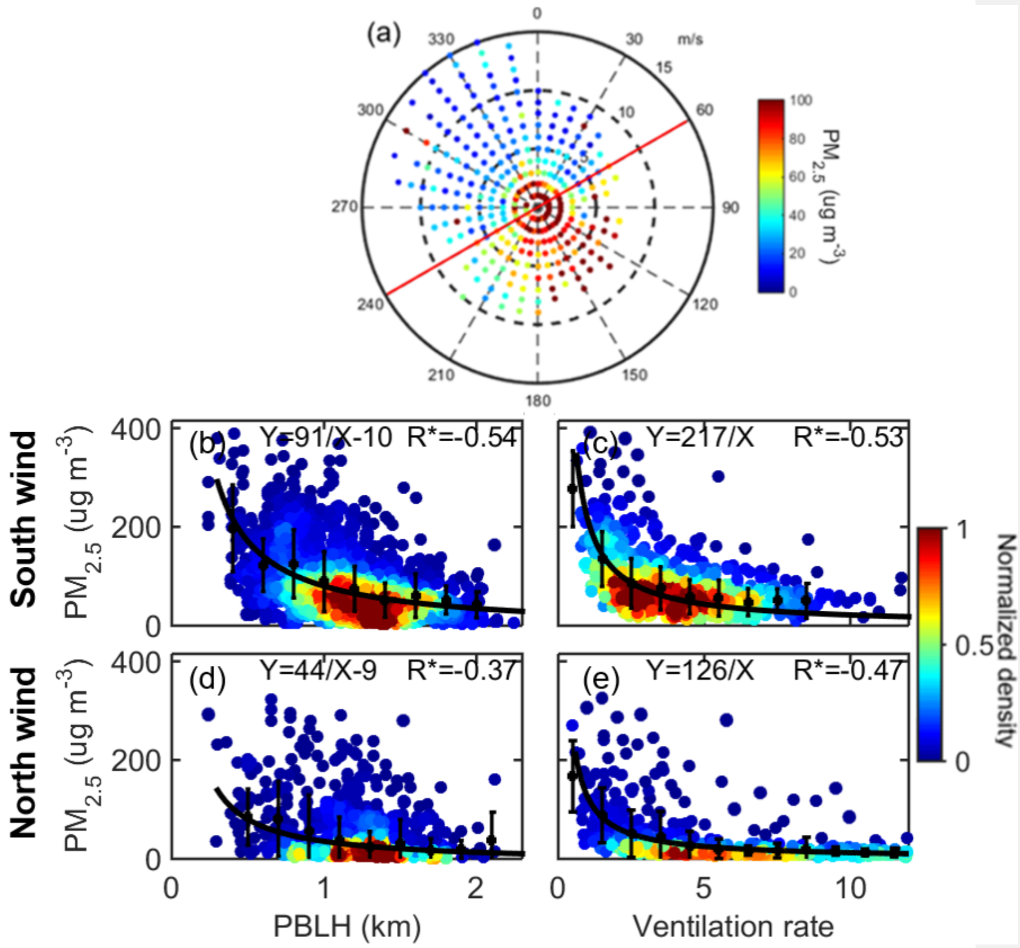

Figure ~~7~~10. (a) Relationship between wind direction/wind speed and $PM_{2.5}$ over Beijing. The red line divides the northerly wind and southerly wind. (b-c) The relationship between $PM_{2.5}$ and MPL-PBLH/ventilation rate (VR = WS × PBLH, unit: km*m s^{-1}), for southerly winds over Beijing. (d-e) The relationship between $PM_{2.5}$ and MPL-PBLH/VR, for northerly winds over Beijing.

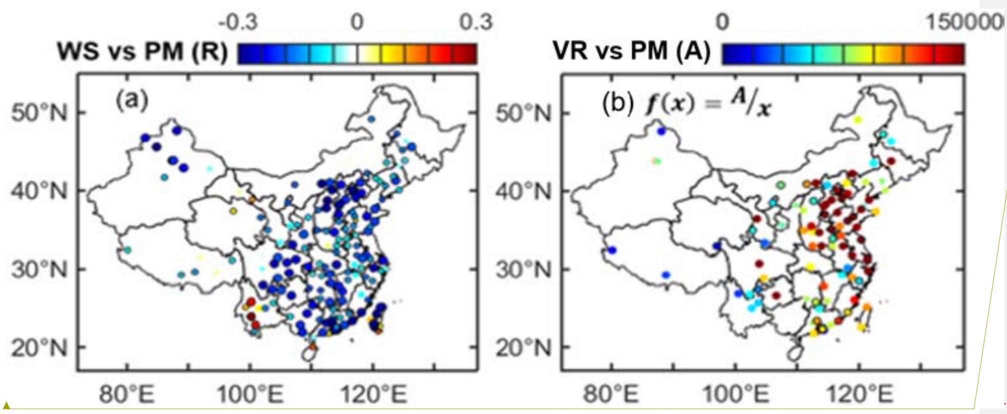

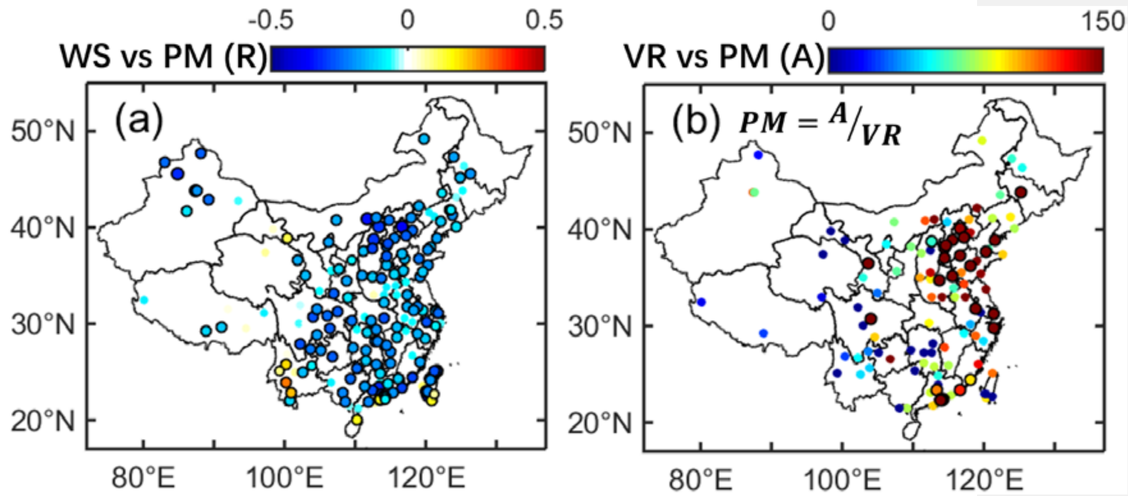

Figure ~~8~~11. (a) Spatial distribution of linear correlation coefficients (R) for the WS-$PM_{2.5}$ relationship. (b) Spatial distribution of fitting parameter (A) for the VR-$PM_{2.5}$ relationship. The function $PM_{2.5}$ ~~$f(x)$~~ $= A/VR$ ~~x~~ is used to characterize the relationship between VR and $PM_{2.5}$, with A (unit: km*ug m^{-3}) as the fitting parameter~~, and x is VR, and $f(x)$ is $PM_{2.5}$~~. Both WS and $PM_{2.5}$ are obtained from surface data, and PBLH are derived from CALIPSO. Here and in the following analysis, ~~Dots~~ dots marked with black circles indicate where the relationship is statistically significant at the ~~95~~99% confidence level.

Formatted: Font: 10 pt

Comment [ZL20]: Just use the terms in the equation !

Comment [ST21]: Changed it in the figure

Comment [ZL22]: Hardly find any. Need to make them more striking

Comment [ST23]: I replot it in the figure

1011 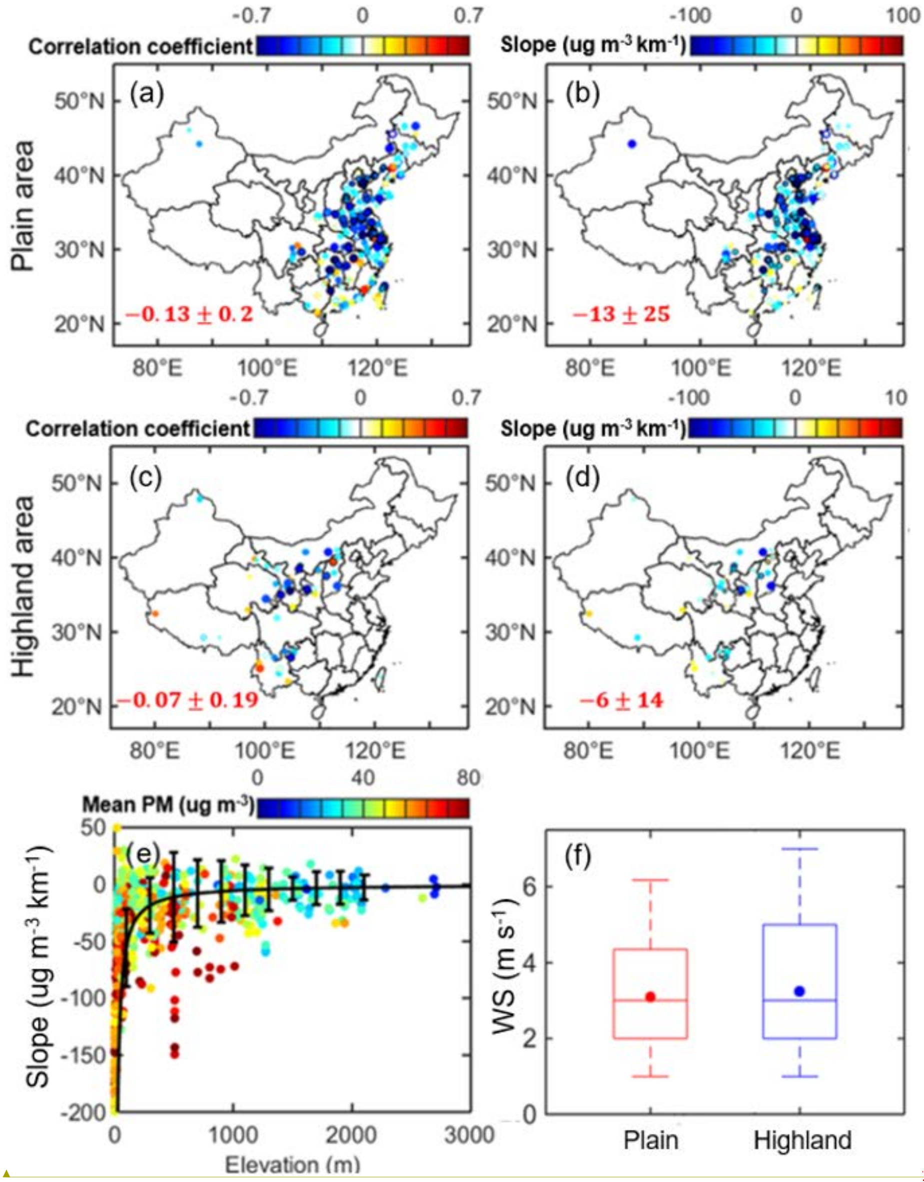

56

Formatted: Font: 10 pt

Formatted: Centered

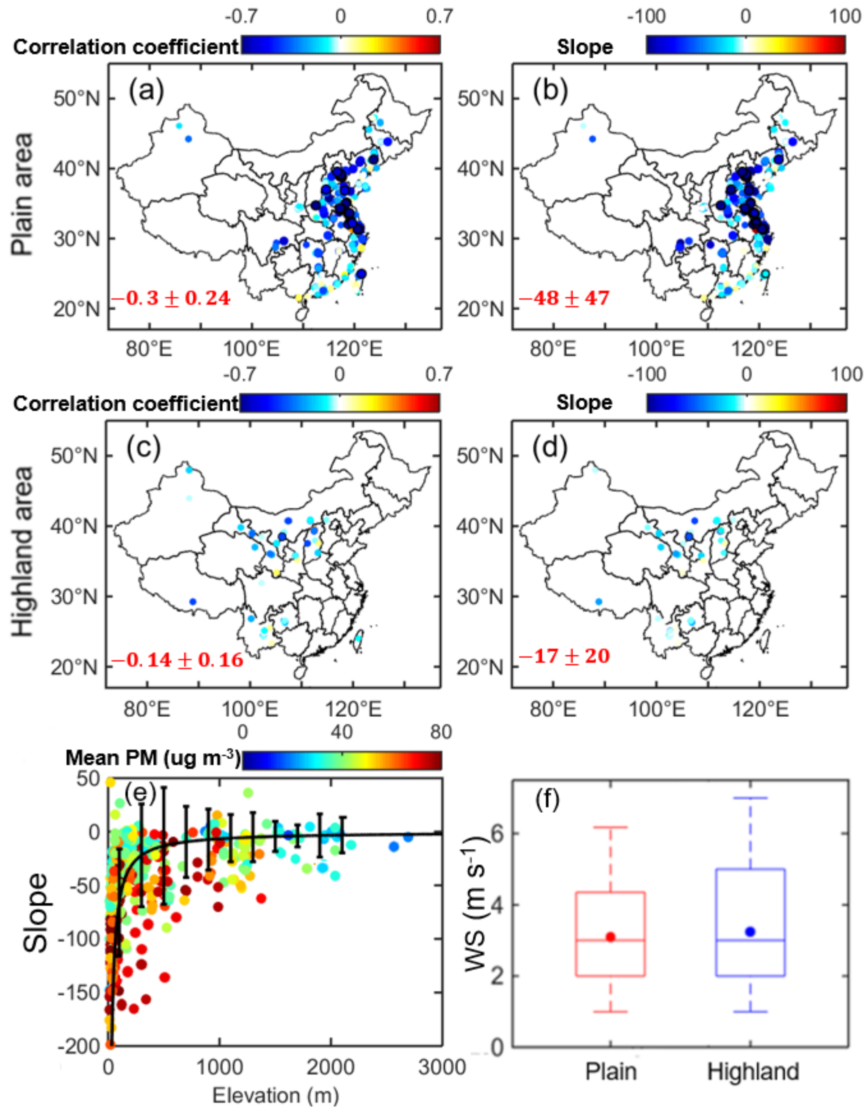

Figure 912. Stratification by terrain elevation. The correlation coefficients (R) and slopes between CALIPSO PBLH and noontime mid-day $PM_{2.5}$ for the plains areas (a-b) and highland areas (c-d). (e) The relationship between PBLH- $PM_{2.5}$ slope and station elevation, with color shading indicating station mean $PM_{2.5}$ concentration. (f) Box and whisker plots showing the 10th, 25th, 50th, 75th, and 90th percentile values of the noontime mid-day WS for plain and highland regions. The dots indicate the mean values.

Stratification by terrain elevation. The correlation coefficients (R) and slopes (unit: km*ug m^{-3})

between CALIPSO PBLH and~~ mid-day ~~ $PM_{2.5}$ ~~derived from~~for the inverse fit~~ting method~~ ($f(x) = {}^{A}/_{x} + B$) are shown for the (a-b) plains ~~(a-b)~~ and (c-d) highland areas~~ (c-d)~~. Noted the slope in the inverse fit is defined as $-A$. (e) The slopes in the inverse fit ~~The relationship between PBLH-$PM_{2.5}$ slope~~ (i.e. linear slopes between $-\frac{1}{\mathrm{PBLH}}$ and $PM_{2.5}$) ~~(derived from~~under different ~~the inverse fitting)~~ ~~and~~ station elevations, with color-shading indicating station mean $PM_{2.5}$ concentration. (f) Box-and-whisker plots showing the 10th, 25th, 50th, 75th, and 90th percentile values of the early-afternoon~~mid-day~~ WS for plain and highland regions. The dots indicate the mean values.

Formatted: Font: 10 pt

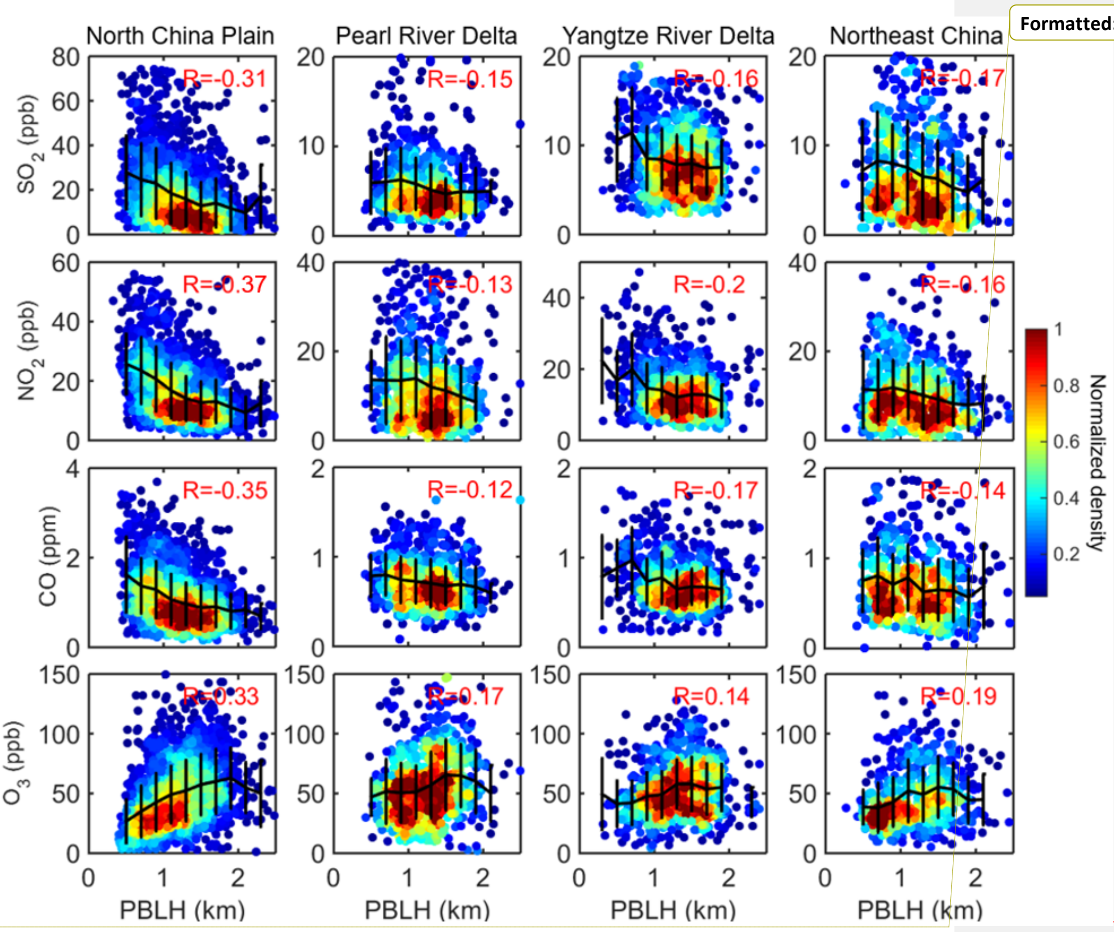

~~**Figure 10.** The relationships between CALIPSO-derived PBLH and multiple gas pollutants over (from left to right) the NCP, PRD, YRD, and NEC. The color shaded dots indicate the normalized sample~~

density. Correlation coefficients (R) are shown in red in each panel.

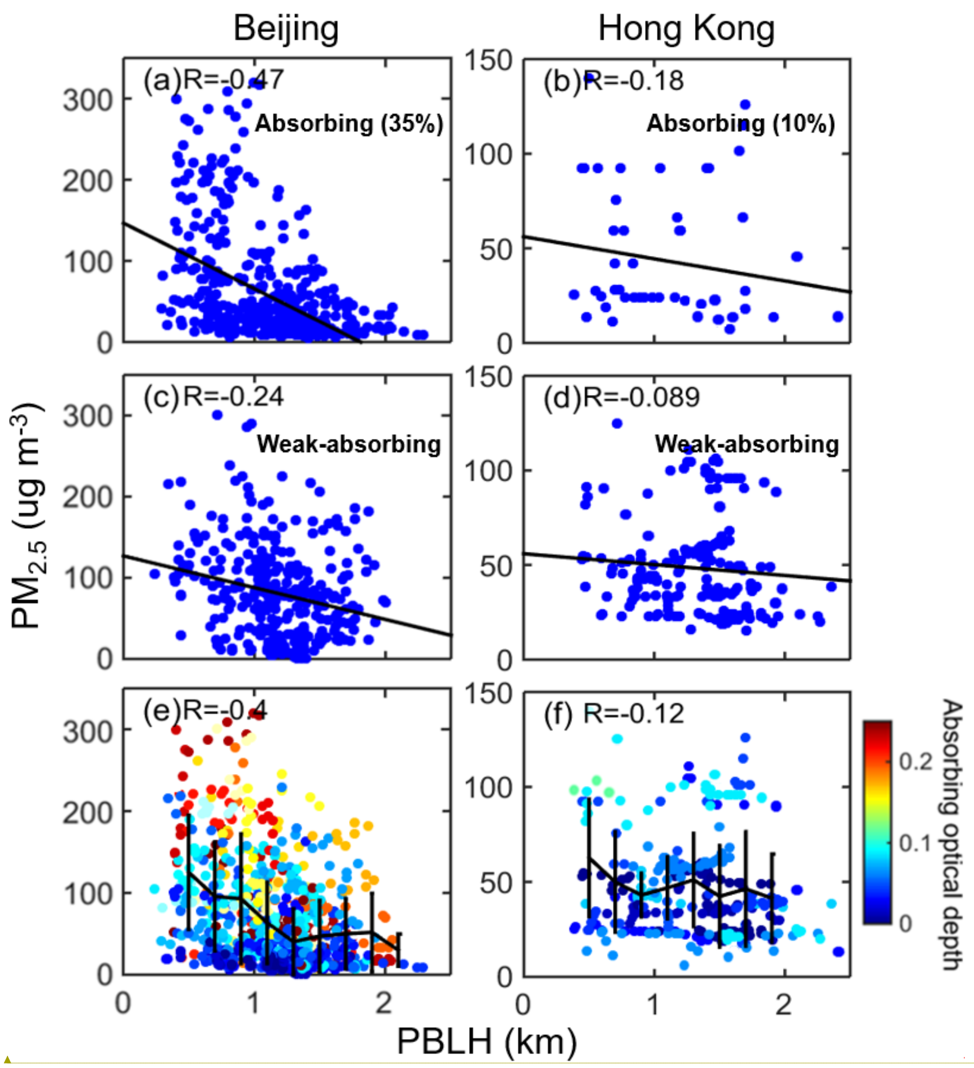

Formatted: Font: 10 pt

Figure 11. The relationship between $PM_{2.5}$ and PBLH for absorbing aerosols over (a) Beijing and (b) Hong Kong. The percentage of absorbing cases are noted in (a) and (b). The relationship between $PM_{2.5}$

and PBLH for weakly absorbing aerosols over (c) Beijing and (d) Hong Kong. In (a, b, c, d), color bars represent normalized density. The relationship between total $PM_{2.5}$ and PBLH over (e) Beijing and (f) Hong Kong. In (e, f), the color shaded dots indicate absorbing optical depth. The PBLHs over Beijing are obtained from MPL, and the PBLHs over Hong Kong are calculated by CALIPSO.